Reviews in Mineralogy, 37, 639-671, 1998

Chapter 19

THEORY OF MINERALS AT HIGH PRESSURE

Lars Stixrude

Department of Geological Sciences
425 E. University Ave.
University of Michigan
Ann Arbor, Michigan 48109

Ronald E. Cohen and Russell J. Hemley

Geophysical Laboratory and Center for High Pressure Research
Carnegie Institution of Washington
5251 Broad Branch Rd. NW
Washington, D.C. 20015

INTRODUCTION

Recent studies of minerals at very high pressures are yielding numerous surprises that present a considerable challenge to our understanding of mineral structure and bonding. In the context of earth sciences, the exploration of high pressure has opened up mineralogy to the investigation of the bulk of our planet that lies beneath the surface. The earth's interior is a unique environment in which the behavior of minerals often overturns our textbook intuition. Primarily because in situ experimental studies of minerals over the entire range of conditions encountered within the Earth are so new and just now being explored, the nature and evolution of the earth's interior is poorly understood, and difficult to predict with current theoretical understanding. In contrast, we have a better understanding in many ways of the interiors of distant stars. For example, we are able to calculate the structures and evolutionary history of stars with some certainty, an exercise that is not yet possible for the earth. The reason is that, because the pressure is so high, the electrons obey an almost trivial limiting behavior, the uniform electron gas (Ichimaru 1982). The underlying physics is that the kinetic energy of electrons increases with the charge density, ρ, as $\rho^{2/3}$ while the potential energy binding the electrons to the nuclei increases only as $\rho^{1/3}$; the kinetic energy dominates at high pressure and the electrons become unbound (see Bukowinski 1994 for an extended discussion).

The contrast with planetary interiors can be illustrated by expressing the pressure in terms of atomic units, one atomic unit (29.4 TPa) being comparable to the pressure required for complete ionization and the formation of a degenerate electron gas. The structure of planets are such that pressures are much less than unity. The behavior of planetary materials will be far from plasma-like, and therefore much more complex; the pressure-temperature domain is such that materials are best described as condensed matter. Using other language, although chemical effects are still dominant (i.e. properties controlled by the orbital structure of atoms), strong perturbations of these properties can introduce new and unsuspected complexity. A more useful pressure scale in the context of planetary interiors is formed from an energy typical of the spacing between electronic bands (1 eV) and a volume typically occupied by a valence electron in a mineral (20 $Bohr^3 \approx 3$ $Å^3$). This pressure scale (~50 GPa) is characteristic of the earth's interior and of the bulk modulus of typical earth-forming constituents. On quite general grounds we must expect to find in planetary interiors not only significant compression and phase transitions, but also

0275-0279/98/0037-0019$05.00

electronic transitions (e.g. insulator to metal) and substantial changes in the mechanisms of bonding, all of which complicate our picture of planetary structure and evolution.

The recognition that minerals at high pressure are characterized by complex multi-phase behavior places tremendous demands on the required accuracy of theoretical methods. They must be general, applicable to essentially all classes of elements, and must not make any assumptions regarding the nature of bonding. This generality rules out most semi-empirical approaches that are based on our more traditional notions of mineral behavior, such as the otherwise powerful ionic model. Moreover, energies and volumes must be accurate to well within typical heats and volumes of solid-solid transformations, ruling out essentially all weak screening approaches that treat condensed matter in perturbative fashion beginning with the free electron gas. Indeed, early calculations using one such approach (Jensen 1938) incorrectly predicted that iron is substantially less dense than the earth's core (Birch 1952). On the other hand, the goal of theory is not only to provide accurate quantitative predictions of physical properties that can be measured experimentally (at least in principle); theory should provide important physical insight and understanding into phenomena that may not be apparent from measurements or from large-scale computations. Thus, the simpler approaches play an important role in providing this insight.

Over the past decade or so, theoretical methods have been developed that have sufficient generality and power to tackle the complex behavior we expect to find in high-pressure mineralogy. These first-principles methods are relatively new to the earth sciences literature and have not been widely reviewed. Moreover, unlike more venerable semi-empirical or ab initio models, they are based on a microscopic view of minerals that differs radically from our traditional intuition. This review explores some of the theoretical methods that have been applied in high-pressure mineralogy, but focuses on first-principles methods because of their relative historical and conceptual novelty. The following sections review in some detail modern first-principles methods based on density functional theory as they have been applied in the earth science literature, and the fundamental approximations upon which these methods are based. First-principles methods are contrasted with those ab initio and semi-empirical models that have also played an important role. We then discuss the derivation of observable quantities from density functional theory, and briefly review computational methods for solving the equations. Finally, we discuss applications of theory to understanding and predicting the behavior of minerals deep within the Earth, and explore some important unsolved problems and possible future directions.

THEORY

A wide range of theoretical methods have appeared in the earth sciences literature, and many have been applied to understanding the behavior of deep Earth materials. These methods differ vastly in the level of physics included and as a result in the quality and security of their predictions. Two extremes of the theoretical spectrum—semi-empirical to first principles—reflect two superficially different views of the microscopic world. The empirically-based ionic model, originally developed by Goldschmidt and Pauling (1960), forms the foundation of much of our understanding of mineral behavior. It continues to play an important conceptual role and forms the basis of most modern semi-empirical atomistic approaches. However, our traditional mineralogical intuition often fails us in the very high-pressure environment. The marked changes in electronic properties of materials that can occur under these extreme conditions require new approaches. First-principles methods view minerals in a very different way which, being more closely tied to the fundamental physics, permits understanding and prediction of unique high pressure behavior. This review focuses primarily on the first-principles approach as embodied in density functional theory by exploring it with semi-empirical and ab initio models of mineral structure and bonding.

From the point of view of any first and electrons; atoms and ions are constru our usual way of thinking about miner consequences. We may expect our theo conditions encountered in planets (a environments entailed by this enormous elements of the periodic table.

To illustrate this way of thinking concepts, we consider first the properties with embedded nuclei. The total energy c three distinct contributions to the potenti and electrons (2) electron exchange and straightforward and involves only sums c charge density. The latter two are corre which is invoked to render the full N-bo appear) tractable.

Exchange and correlation account f from the tendency of electrons to avoic Coulomb repulsion, whereas exchange resulting tendency of electrons of the sa each electron can be thought of as diggi Certain properties of the exchange-corr instance that its integrated charge must e correlation reduce the total energy by red

The total energy of our simple sys density; the equation of state then follow in a close-packed arrangement, and contributions to exchange and correlatio

$$P = 0.176 r_s^5 \left[1 - \left(0.407 Z^{2/3} + 0.2\right.\right.$$

where P is the static (athermal) pressure,

$$r_s = \left(\frac{3}{4\pi\rho}\right)^{1/3}$$

is a measure of the average spacing betw kinetic contribution, the second due to th and mutual repulsion of the electrons, smaller than exchange at high density, repulsion of the nuclei.

Comparisons with the structure o important aspects of planetary matter (electrons by the nuclei plays an essential charges account to first order for the diff Jupiter and earth. Second, screening h

density functional theory by exploring its properties and capabilities and by contrasting it with semi-empirical and ab initio models that are more closely tied to our traditional views of mineral structure and bonding.

From the point of view of any first principles theory, solids are composed of nuclei and electrons; atoms and ions are constructs that play no primary role. This departure from our usual way of thinking about minerals is essential and has the following important consequences. We may expect our theory to be equally applicable to the entire range of conditions encountered in planets (and even stars), the entire range of bonding environments entailed by this enormous range of pressures and temperatures, and to all elements of the periodic table.

To illustrate this way of thinking about solids and to introduce some important concepts, we consider first the properties of the simplest system, the uniform electron gas with embedded nuclei. The total energy consists of the kinetic energy of the electrons, and three distinct contributions to the potential energy: (1) Coulomb interactions among nuclei and electrons (2) electron exchange and (3) electron correlation. The first contribution is straightforward and involves only sums over point charges and integrals over the electronic charge density. The latter two are corrections to the independent electron approximation which is invoked to render the full N-body problem (in which only Coulomb interactions appear) tractable.

Exchange and correlation account for local deviations from uniform charge that arise from the tendency of electrons to avoid each other. Correlation accounts for the mutual Coulomb repulsion, whereas exchange embodies the Pauli exclusion principle and the resulting tendency of electrons of the same spin to avoid each other. The net effect is that each electron can be thought of as digging a hole of reduced charge density about itself. Certain properties of the exchange-correlation hole are well understood; it is known for instance that its integrated charge must exactly balance that of the electron. Exchange and correlation reduce the total energy by reducing the Coulomb repulsion between electrons.

The total energy of our simple system is readily evaluated as a function of charge density; the equation of state then follows from differentiation. Assuming that the nuclei are in a close-packed arrangement, and including only the leading order high density contributions to exchange and correlation, the equation of state is (Hubbard 1984)

$$P = 0.176 r_s^5 \left[1 - \left(0.407 Z^{2/3} + 0.207 \right) r_s \right] \tag{1}$$

where P is the static (athermal) pressure, Z the nuclear charge, and the Wigner-Seitz radius

$$r_s = \left(\frac{3}{4\pi\rho} \right)^{1/3} \tag{2}$$

is a measure of the average spacing between electrons. The first term in Equation (1) is the kinetic contribution, the second due to the Coulomb attraction of the nuclei for the electrons and mutual repulsion of the electrons, and the third to exchange. Correlation, which is smaller than exchange at high density, has been neglected as has the mutual Coulomb repulsion of the nuclei.

Comparisons with the structure of planetary interiors reveal some fundamentally important aspects of planetary matter (Fig. 1). First, the net Coulomb attraction of the electrons by the nuclei plays an essential role at planetary densities—different mean nuclear charges account to first order for the difference in mean charge (and mass) density between Jupiter and earth. Second, screening has a first order effect on the equation of state,

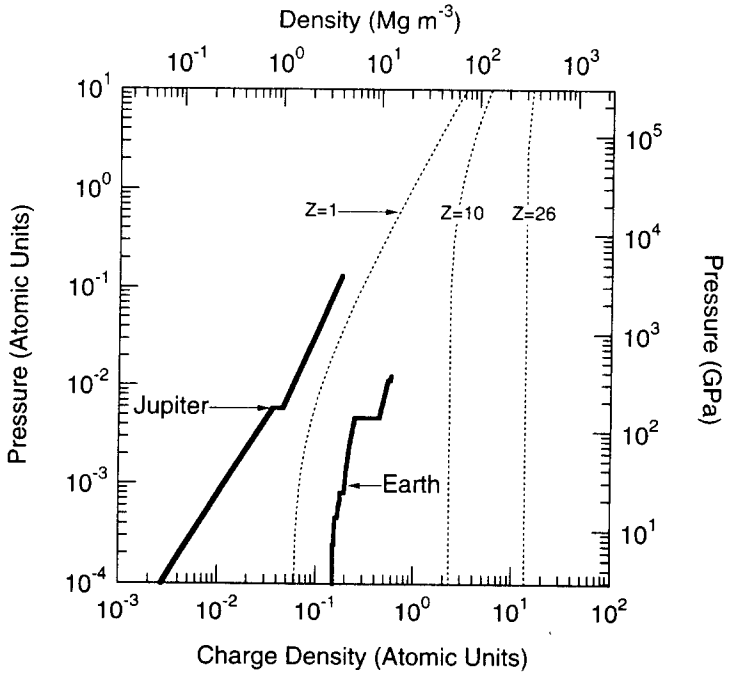

Figure 1. Pressure in the interior of Jupiter (Chabrier 1992) and earth (Dziewonski and Anderson 1981) as a function of mass density (top) and charge density (bottom). The charge density has been calculated from the observed mass density by assuming that the number of electrons is one-half the number of nucleons. Planetary structures are compared with limiting high density equations of state (Eqn. 1) for three values of the atomic number, Z.

accounting for the much lower densities of planets at a given pressure than predicted by Equation (1). In planetary matter, the charge density is substantially enhanced in the vicinity of the nucleus, reducing the ability of the point charges to attract the remaining (valence) electrons. Screening is weaker in the case of Jupiter because it contains dominantly lighter elements, and because the pressures are much greater. Nevertheless, for all the planets screening is so strong that it must be accounted for. The major part of the screening is from the tightly bound, essentially rigid core electrons. In the case of the terrestrial planets, the charge density near the nuclei is so much higher than in the interstitial region that this difference plays a central role in the design of modern computational methods.

First-principles level

We turn now from simple to real systems and at the same time from analytically expressible results to necessarily elaborate computations. Though the electronic structure will be non-trivial, we retain the charge density as a central concept. This is appealing because this quantity is experimentally observable; it is precisely what is measured by an x-ray diffraction experiment. While we will focus on density functional theory here, there are other first-principles methods that have been important in the earth science literature; among these is the periodic Hartree-Fock method (Dovesi et al. 1987). What all first-principles methods share is an approach that seeks to minimize approximations to the bare minimum. Some approximation is necessary since we are as yet incapable of solving the Schrödinger equation exactly for any mineralogical system.

Density functional theory. T
uniform, non-degenerate electron syste
the positions of the nuclei, we mus
wavefunction, $\Psi(r_1,r_2,\ldots,r_N)$ of a syst
order of Avagadro's number. Density fu
and Sham 1965) is a powerful and in pri
a tractable way (see Lundqvist and Mar

The essence of this theory is the pr
a unique functional of the charge density
total energy

$$E = T + U[\rho(\vec{r})] + E_{xc}[\rho(\vec{r})]$$

and its derivatives (pressure, elastic c
system of non-interacting electrons with
U is the electrostatic (Coulomb) energy
nuclei, and E_{xc} is the exchange-correlat
single-particle, Schrödinger- like, Kohn

$$\left[-\nabla^2 + V_{KS}\right]\psi_i = \varepsilon_i\psi_i$$

where ψ_i is now the wave function of a
the effective potential

$$V_{KS}[\rho(\vec{r})] = \sum_{i=1}^{N}\frac{2Z_i}{\left|\vec{r}-\vec{R}_i\right|} + \int\frac{2\rho(\vec{r}$$

where the first two terms are Coulomb
respectively, the last is the exchange-cor
units: $\hbar^2/2m = 1$, $e^2 = 2$, energy in Ry, a

The power of density functional th
the exact many-body total energy of a
solution to the Kohn-Sham equations is
equations

$$H_{ij}(\vec{k})\psi_j(\vec{r},\vec{k}) = \varepsilon_i(\vec{k})O_{ij}(\vec{k})\psi_j$$

$$H_{ij}(\vec{k}) = \int\psi_i^*(\vec{r},\vec{k})\left(-\nabla^2 + V_{KS}\right)\psi$$

$$O_{ij}(\vec{k}) = \int\psi_i^*(\vec{r},\vec{k})\psi_j(\vec{r},\vec{k})d\vec{r}$$

where **H** and **O** are the Hamiltonian and
reciprocal space. Because the Kohn-Sha
the equations must be solved self-cons
density in terms of the wavefunctions

$$\rho(\vec{r}) = \int\sum_i n(E_F-\varepsilon_i)\psi_i^*(\vec{r},\vec{k})\psi$$

where n is the occupation number, and

Density functional theory. The general problem we are faced with in a non-uniform, non-degenerate electron system is formidable. Given a periodic potential set by the positions of the nuclei, we must solve the Schrödinger equation for the total wavefunction, $\Psi(r_1,r_2,\ldots,r_N)$ of a system of N interacting electrons, where N is on the order of Avagadro's number. Density functional theory (Hohenberg and Kohn 1964, Kohn and Sham 1965) is a powerful and in principle exact method of dealing with this problem in a tractable way (see Lundqvist and March 1987 for reviews).

The essence of this theory is the proof that the ground state properties of a material are a unique functional of the charge density $\rho(\vec{r})$. Among these properties are the ground state total energy

$$E = T + U[\rho(\vec{r})] + E_{xc}[\rho(\vec{r})] \tag{3}$$

and its derivatives (pressure, elastic constants, etc.) where T is the kinetic energy of a system of non-interacting electrons with the same charge density as the interacting system, U is the electrostatic (Coulomb) energy, including the electrostatic interaction between the nuclei, and E_{xc} is the exchange-correlation energy. A variational principle leads to a set of single-particle, Schrödinger- like, Kohn-Sham equations

$$\left[-\nabla^2 + V_{KS}\right]\psi_i = \varepsilon_i \psi_i \tag{4}$$

where ψ_i is now the wave function of a single electron, ε_i the corresponding eigenvalue and the effective potential

$$V_{KS}[\rho(\vec{r})] = \sum_{i=1}^{N} \frac{2Z_i}{\left|\vec{r} - \vec{R}_i\right|} + \int \frac{2\rho(\vec{r}')}{\left|\vec{r} - \vec{r}'\right|} d\vec{r}' + V_{xc}[\rho(\vec{r})] \tag{5}$$

where the first two terms are Coulomb potentials due to the nuclei and the other electrons, respectively, the last is the exchange-correlation potential, and the units are Rydberg atomic units: $\hbar^2/2m = 1$, $e^2 = 2$, energy in Ry, and length in Bohr.

The power of density functional theory is that it allows one to calculate, in principle, the exact many-body total energy of a system from a set of single-particle equations. The solution to the Kohn-Sham equations is that of the set of coupled generalized eigenvalue equations

$$H_{ij}(\vec{k})\psi_j(\vec{r},\vec{k}) = \varepsilon_i(\vec{k}) O_{ij}(\vec{k})\psi_j(\vec{r},\vec{k}) \tag{6}$$

$$H_{ij}(\vec{k}) = \int \psi_i^*(\vec{r},\vec{k})\left(-\nabla^2 + V_{KS}\right)\psi_j(\vec{r},\vec{k})d\vec{r} \tag{7}$$

$$O_{ij}(\vec{k}) = \int \psi_i^*(\vec{r},\vec{k})\psi_j(\vec{r},\vec{k})d\vec{r} \tag{8}$$

where **H** and **O** are the Hamiltonian and overlap matrices, respectively and $\vec{k}$ is a vector in reciprocal space. Because the Kohn-Sham potential is a functional of the charge density, the equations must be solved self-consistently together with the definition of the charge density in terms of the wavefunctions

$$\rho(\vec{r}) = \int \sum_i n(E_F - \varepsilon_i)\psi_i^*(\vec{r},\vec{k})\psi_i(\vec{r},\vec{k})d\vec{k} \tag{9}$$

where n is the occupation number, and E_F is the Fermi energy.

Approximations. The Kohn-Sham equations are exact. That only approximate solutions have been possible to date is a limitation imposed only by our current ignorance of the exact exchange-correlation functional. If the exact exchange-correlation functional were known, we would be able to obtain exact solutions. All other terms in the Kohn-Sham equations are straightforward and readily evaluated. In addition to the essential approximation to the exchange-correlation potential, two other approximations are commonly invoked in some first principles calculations: the frozen-core approximation and the pseudopotential approximation. These three approximations are now discussed in detail:

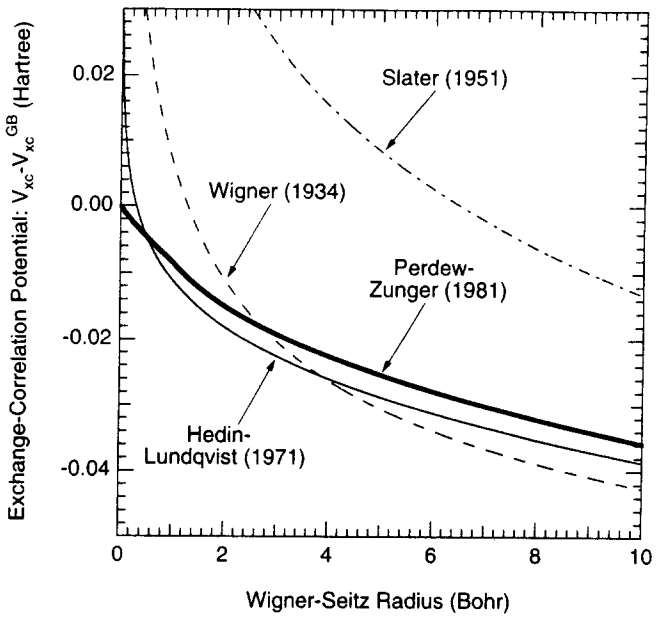

Figure 2. The difference between the exchange-correlation potential and its high-density limit (Eqns. 10,11) in (bold line) the local density approximation (LDA), and (other lines) three commonly used approximations to the LDA (Hedin and Lundqvist 1971, Slater 1951, Wigner 1934). For the Slater result, we use $\alpha = 2/3$ which yields the pure exchange potential.

The exchange-correlation potential. The exchange-correlation functional is known precisely only for simple systems such as the uniform electron gas (Fig. 2). The exchange portion is known analytically, as are the leading order contributions to correlation, in the limit of high density (Gell-Mann and Brueckner 1957)

$$V_{xc} = \frac{\partial}{\partial \rho}[\rho E_{xc}] \tag{10}$$

$$E_{xc} = -\frac{3}{4\pi}\left(\frac{9\pi}{4}\right)^{1/3} r_s^{-1} + A \ln r_s + B \tag{11}$$

where E_{xc} is the exchange-correlation energy, the first contribution to E_{xc} is exchange, and the constants, $A = (1\text{-}\ln 2)/\pi^2$ and $B = -0.046644$ (Perdew et al. 1996). At other densities, accurate values of the exchange-correlation potential are known from quantum Monte Carlo calculations (Ceperley and Alder 1980), which have been represented in a parametric form

that obeys the high density limiting bel

The precision of modern conder representation of the exchange-correlati issue. In this context, one must be a appeared frequently in the geophysical Lundqvist (1971) expression is most ization, that of Wigner (1934) the least. dependence on density than the accurat functional computations for solids. Nc satisfy the correct high-density limiting

The charge density in real mat correlation potential cannot be evalu exchange-correlation potential have b mation (LDA) is based on the uniform lowest order by setting V_{xc} at every pc with a density equal to the local charge

The success of the LDA can be satisfaction of exact sum rules for Lundqvist 1976). For example, the LD unit charge. Ultimately, the appropriat its predictions to observation. Here, th has been shown to yield excellent a insulators, metals, and semiconductors also shows some important flaws; for e iron. It also shows failures in the trans where insulating ground states are obse

These failures have prompted functionals. One shortcoming of the LI distinguish between electrons of differe approximations (GGA) partially reme density gradients in addition to the den gradient approximations; a straightforv gradient about the LDA result fails exchange-correlation hole. The most satisfies the sum rules exactly (Perdew have been shown to yield agreement wi and often substantially better (Perdew the bcc phase as the ground state of however: for some materials, LDA resu transition metals (Körling and Häglu failure of LDA in the case of the transit LDA can be expressed in terms of the e

$$F(r_s, s) = \frac{V_{xc}^{GGA}(r_s, s)}{V_x(r_s)}$$

where V_x is the exchange potential an dimensional charge density gradient $s =$

that obeys the high density limiting behavior (Eqns. 10, 11) (Perdew and Zunger 1981).

The precision of modern condensed-matter computations have made the accurate representation of the exchange-correlation potential of the uniform electron gas an important issue. In this context, one must be aware that approximate representations of V_{xc} have appeared frequently in the geophysical literature and are still in use. Of these, the Hedin-Lundqvist (1971) expression is most similar to the accurate Perdew-Zunger parameterization, that of Wigner (1934) the least. The Wigner approximation shows a much stronger dependence on density than the accurate potential, and leads to significant errors in density functional computations for solids. None of the commonly used approximate expressions satisfy the correct high-density limiting behavior (Eqns. 10, 11).

The charge density in real materials is highly non-uniform, and the exchange-correlation potential cannot be evaluated. Fortunately, simple approximations to the exchange-correlation potential have been very successful. The Local Density Approximation (LDA) is based on the uniform electron gas, taking into account nonuniformity to lowest order by setting V_{xc} at every point in the crystal to that of the uniform electron gas with a density equal to the local charge density (Lundqvist and March 1987).

The success of the LDA can be understood at a fundamental level in terms of the satisfaction of exact sum rules for the exchange-correlation hole (Gunnarsson and Lundqvist 1976). For example, the LDA correctly predicts an exchange-correlation hole of unit charge. Ultimately, the appropriateness of the LDA can be judged only by comparing its predictions to observation. Here, the LDA has been remarkably successful. The LDA has been shown to yield excellent agreement with experiment for a wide variety of insulators, metals, and semiconductors, for bulk, surface, and defect properties. The LDA also shows some important flaws; for example, it fails to predict the correct ground state of iron. It also shows failures in the transition metal oxides, predicting metallic ground states where insulating ground states are observed.

These failures have prompted the development of new exchange-correlation functionals. One shortcoming of the LDA may be its local character, that is, its inability to distinguish between electrons of different angular momenta or energy. Generalized gradient approximations (GGA) partially remedy this by including a dependence on local charge density gradients in addition to the density itself. Some care must be taken in constructing gradient approximations; a straightforward Taylor series expansion in the charge density gradient about the LDA result fails completely since it violates the sum rule for the exchange-correlation hole. The most widely used generalized gradient approximation satisfies the sum rules exactly (Perdew et al. 1996). This approximation and its forerunners have been shown to yield agreement with experimental data that is usually as good as LDA and often substantially better (Perdew et al. 1992). For example, GGA's correctly predict the bcc phase as the ground state of iron (Bagno et al. 1989). GGA is not a panacea however: for some materials, LDA results are in better agreement with experiment, e.g. 5d transition metals (Körling and Häglund 1992). Moreover, GGA does not alleviate the failure of LDA in the case of the transition metal oxides. The relationship of the GGA to the LDA can be expressed in terms of the enhancement factor

$$F(r_s, s) = \frac{V_{xc}^{GGA}(r_s, s)}{V_x(r_s)} \tag{12}$$

where V_x is the exchange potential and F is a function of the charge density and the non-dimensional charge density gradient $s = 24/\pi^2 \left| \nabla\rho/\rho^{4/3} \right|$ (Fig. 3).

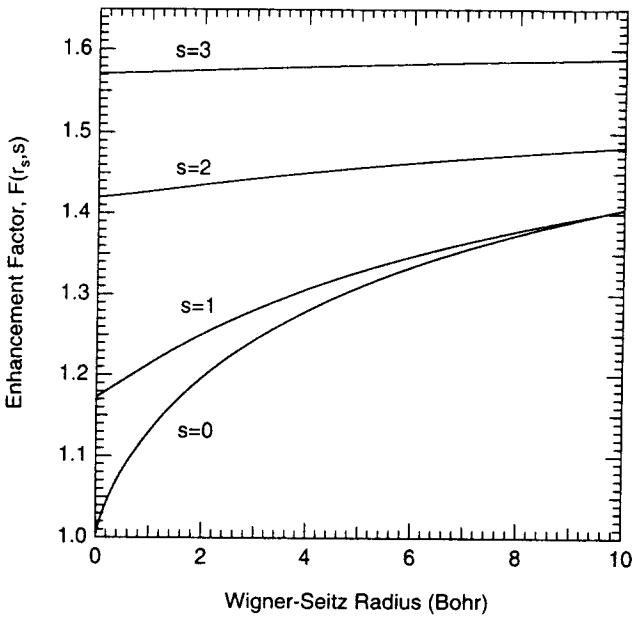

Figure 3. The effect of charge-density gradients on the exchange-correlation potential according to the generalized gradient approximation (GGA). The enhancement factor for zero gradient ($s = 0$) reflects the contribution of correlation to V_{xc}.

The frozen core approximation. The physical motivation for this approximation is the observation that only the valence electrons participate in bonding and in the response of the crystal to most perturbations of interest. Unless the perturbation is of very high energy (comparable to the binding energy of the core states), the tightly bound core states remain essentially unchanged. The frozen core approximation is satisfied to a high degree of accuracy for many applications, for example in the case of finite strains of magnitudes typically encountered in the earth's interior.

Within this approximation, the charge density of the core electrons is just that of the free atom, which can be found readily. We then need solve only for the valence electrons in Equation (4), often a considerable computational advantage. An important technical point is that, although in many cases the choice is obvious, there is no fundamentally sound way to decide *a priori* which electrons are core and which valence. Some care is required; for example, the 3p electrons in iron must be treated as valence electrons as they are found to deform substantially at pressures comparable to those in the earth's core (Stixrude et al. 1994).

The pseudopotential approximation. This approximation goes one step beyond the frozen core. It replaces the nucleus and the core electrons with a simpler object, the pseudopotential, that has the same scattering properties (Pickett 1989). The pseudopotential is chosen such that the valence wave function in the free atom is the same as the all electron solution beyond some cutoff radius, but nodeless within this radius. The advantages of the pseudopotential method are (1) spatial variations in the pseudopotential are much less rapid than the bare Coulomb potential of the nucleus and (2) one need solve only for the (pseudo-) wavefunctions of the valence electrons which show much less rapid spatial variation than the core electrons, or the valence electrons in the core region. This means that

in the solution of the Kohn-Sham
represented by a particularly simple, c
waves) of manageable size. With this
forces acting on the atoms is particular

The pseudopotential is an appro
"see" and its construction is non-uniq
different predictions of bulk prope
pseudopotentials have been develope
Vanderbilt 1990). Care must be take
potentials generated by a particular m
where these are available. When the
potential is generally small (few percer

Ab initio models

Whereas first-principles methods
ab initio models construct an appro
physics, such as the charge density
additional approximation is often outw
and efficiency. For example, ab initio
properties or the properties of liquids w
first-principles approaches. Moreover
difficult to extract from more complex

Gordon-Kim type approach
Gordon and Kim (1972) bridges the g
density functional theory. While based
shell atoms or ions, it shows the pow
approximation even when these are no
charge density self-consistently with t
overlapping atomic or ionic charge den
charge density using the LDA. This
because the charge density of isola
consistency is not enforced. The metho
the Kohn-Sham equations, even if the
form for the kinetic energy is not accu
give the proper shell structure for ato
approximation to the kinetic energy eve
occupied orbitals. In subsequent wo
modified (leading to the term modifie
atoms (Cohen and Gordon 1975, 19
state that are too stiff for the rare g
simplicity of the model. These shortc
partially overcome in the case of rare-g
respond to the embedding crystal poten
pressure (LeSar 1988). However, the
principal interactions, particularly the T
case of MEG) as opposed to the Kohn-

Care must be taken in the treatmen
is unstable in the free state. This diff
Watson sphere which mimics the emb
crystal (Watson 1958). Thus O^{2-} is sur

in the solution of the Kohn-Sham equations, potential and charge density can be represented by a particularly simple, complete and orthogonal set of basis functions (plane-waves) of manageable size. With this basis set, evaluation of total energies, stresses, and forces acting on the atoms is particularly efficient.

The pseudopotential is an approximation to the potential that the valence electrons "see" and its construction is non-unique; different pseudopotentials may yield significantly different predictions of bulk properties. Several different methods for constructing pseudopotentials have been developed (Lin et al. 1993, Troullier and Martins 1991, Vanderbilt 1990). Care must be taken to demonstrate the transferability of the pseudopotentials generated by a particular method and to compare with all electron calculations where these are available. When these conditions are met, the error due to the pseudopotential is generally small (few percent in volume for earth materials).

Ab initio models

Whereas first-principles methods seek to reduce approximations to a bare minimum, ab initio models construct an approximate treatment of some aspects of the relevant physics, such as the charge density or of the interactions between orbitals. The cost of additional approximation is often outweighed by the increase in computational simplicity and efficiency. For example, ab initio models have been widely used to explore transport properties or the properties of liquids which are very difficult (costly) to examine with fully first-principles approaches. Moreover, these models often yield insight that is sometimes difficult to extract from more complex and elaborate first principles calculations.

Gordon-Kim type approaches. This class of approaches, first introduced by Gordon and Kim (1972) bridges the gap between traditional ionic models of minerals and density functional theory. While based on the idea that materials are composed of closed-shell atoms or ions, it shows the power of density functional theory and the local density approximation even when these are not used self-consistently. Instead of solving for the charge density self-consistently with the potential, the total charge density is modeled by overlapping atomic or ionic charge densities and then the total energy is computed for that charge density using the LDA. This approximation leads to much faster computations because the charge density of isolated atoms or ions is easily calculated and self-consistency is not enforced. The method is less accurate than the self-consistent solution to the Kohn-Sham equations, even if the model density is good, because the local density form for the kinetic energy is not accurate enough in many cases (for example it does not give the proper shell structure for atoms). The Kohn-Sham approach does not make this approximation to the kinetic energy even in the LDA and the kinetic energy derives from the occupied orbitals. In subsequent work, the kinetic and correlation interactions were modified (leading to the term modified electron gas, or MEG) to give better results for atoms (Cohen and Gordon 1975, 1976). The MEG model generally gives equations of state that are too stiff for the rare gas solids, but is quite successful considering the simplicity of the model. These shortcomings of the simple Gordon-Kim model can be partially overcome in the case of rare-gas solids by allowing the atomic charge densities to respond to the embedding crystal potential, so that the atom is compressed with increasing pressure (LeSar 1988). However, the principal error arises from the simplicity of the principal interactions, particularly the Thomas-Fermi kinetic energy functional (scaled in the case of MEG) as opposed to the Kohn-Sham approach.

Care must be taken in the treatment of oxides within this approach because the O^{2-} ion is unstable in the free state. This difficulty is overcome by surrounding the ion with a Watson sphere which mimics the embedding crystal potential that stabilizes the ion in the crystal (Watson 1958). Thus O^{2-} is surrounded by a sphere of charge +2: when an electron

moves far from the atom it sees an object of positive charge +1 behind it, the electron is bound and the configuration remains stable. The remaining question is how to choose the radius of the sphere. The original Gordon-Kim calculations of oxides used rigid ion potentials in which the ion was stabilized with a sphere whose radius was chosen so that the electrostatic potential in the sphere was equal to the Madelung potential at the site at a given volume (Muhlhausen and Gordon 1981). In subsequent calculations, an important contribution from the self-energy of the ion was included; this is crucial for predicting volume (i.e. pressure) dependent properties (e.g. Hemley et al. 1985, 1987). This approach was used to study a number of deep mantle minerals at high pressures.

The Potential Induced Breathing (PIB) model represented an extension of this approach (Boyer et al. 1985). It was also introduced to improve the accuracy of elasticity calculations, including the correct prediction of the deviation from the Cauchy conditions (accurate values for the shear and off-diagonal elastic constants, which for rigid ion potentials are equal; e.g. $c_{12}=c_{44}$ for cubic). In this model, the Watson-sphere radius is given by the Madelung potential as atoms are displaced or the lattice strained, $R_{wat}=Z_{wat}/P_{wat}$, giving a non-rigid ion, many-body, potential. The successes of this approach led to the development of the lattice dynamics of the PIB model (Cohen et al. 1987). Reasonable dispersion curves were obtained for the alkaline earth oxides. In the PIB model, the Watson-sphere radii are given by the Madelung potential, but the Madelung potential is not well behaved in the long-wave limit. A better procedure, though somewhat slower, is to optimize the total energy with respect to Watson sphere radii rather than to choose the radius using the Madelung potential (Wolf and Bukowinski 1988). This gives a Watson sphere radius close to that of PIB at zero pressure, but it changes more rapidly with compression than PIB due to the compression of the atom by short-range forces, in addition to the electrostatic crystal field. This model is known as the VIB, or variationally induced breathing, model. For example, anomalous behavior shown by the PIB model is absent in the VIB model. In the VIB model, the LO-TO splitting is the same as given by a rigid ion model, since all atomic deformations are spherical. There is no dipolar charge relaxation. In spite of the absence of atomic polarizability, the VIB model is very accurate and gives results that compare quite well with self-consistent results and experiment. Ab initio models have undergone further development by including the crystal potential in the atomic calculation, and a self-consistency cycle between the atomic densities and the crystal potential (Edwardson 1989, LeSar 1983). In the Self-Consistent Charge Deformation model (SCAD) (Boyer et al. 1997, Stokes et al. 1996) atomic densities are computed in the crystal potential, and states are occupied in order of energy, allowing charge flow between the atoms. The inclusion of non-spherical charge deformations has increased the accuracy of the models, but at the cost of increased complexity.

Tight binding. In its simplest parametric form, as originally formulated by Slater (1954) and extensively illustrated by Harrison (1989), the tight-binding method differs from those described so far in that the charge density does not appear explicitly. In this form of the method, the wavefunctions are constructed from basis functions consisting of atomic-like orbitals. For basis functions $\phi_{i\alpha}(\vec{r}-\vec{R}_i)$, where α labels the type of orbital (e.g. s, p, d, ...), and i labels the atom, the Hamiltonian and overlap matrices consist of elements

$$H_{i\alpha j\beta}(\vec{k}) = \sum_{l=0}^{\infty} exp[i\vec{k} \bullet \vec{R}_{ij}(l)] S_{\alpha\beta}[\hat{R}_{ij}(l)] h_{\alpha\beta}[R_{ij}(l)] \quad (13)$$

$$O_{i\alpha j\beta}(\vec{k}) = \sum_{l=0}^{\infty} exp[i\vec{k} \bullet \vec{R}_{ij}(l)] S_{\alpha\beta}[\hat{R}_{ij}(l)] o_{\alpha\beta}[R_{ij}(l)] \quad (14)$$

where $R_{ij}(l)$ is the distance between the j-th atom in the l-th unit cell, the center approximation, the $h_{\alpha\beta}$ and $o_{\alpha\beta}$ and j run over all atoms in the unit cell that the basis set consists of functions functions $S_{\alpha\beta}$ can be written in term functions, $h_{\alpha\beta}$ and $o_{\alpha\beta}$, are taken to b chosen such that first principles result the wavefunctions or charge densi tremendously, but renders the calculat

The non self-consistency of the t which has not been widely recognized be written

$$E = \int \sum_i \varepsilon_i(\vec{k}) d\vec{k} + F[\rho(\vec{r})]$$

where the first term is a sum over the functional of the charge density, co energy. In non self-consistent calcula zero which must be fixed in order to energy zero in the tight binding metho

$$E = \int \sum_i \varepsilon_i'(\vec{k}) d\vec{k}$$

where the new eigenvalues are shift formulation, the total energy is given s for pair potential repulsive terms w parameters of the tight binding model structures and total energies. This ap properties of a wide variety of monato et al. 1997b). The approach can be silicates but this has not yet been accor

Semi-empirical atomistic models

The primary advantage of thes computationally fast, allowing one to physics than one could otherwise. In m solids as being composed of ions rather appear explicitly. This strictly preclude electronic effects are important, such transitions occur or in which magnetis transferability of semi-empirical mode structures over which the bonding d transferability, semi-empirical potentia accuracy and can lead to useful predict not yet been accessed experimentally materials.

Many of these models can be cast

where $R_{ij}(l)$ is the distance between the i-th atom in the reference unit cell (labeled $l = 0$) and the j-th atom in the l-th unit cell, the $S_{\alpha\beta}$ are functions of direction only and, in the two-center approximation, the $h_{\alpha\beta}$ and $o_{\alpha\beta}$ are functions only of internuclear distance. Indices i and j run over all atoms in the unit cell, and l runs over all unit cells. Under the assumption that the basis set consists of functions with the symmetry of s, p, d, ... atomic orbitals, the functions $S_{\alpha\beta}$ can be written in terms of spherical harmonics. The distance dependent functions, $h_{\alpha\beta}$ and $o_{\alpha\beta}$, are taken to be parametric functions of distance, with parameters chosen such that first principles results are reproduced. In this way, all explicit reference to the wavefunctions or charge density is eliminated. This simplifies the calculations tremendously, but renders the calculation non-self-consistent.

The non self-consistency of the tight binding approach has an important consequence which has not been widely recognized (Cohen et al. 1994). In general, the total energy can be written

$$E = \int \sum_i \varepsilon_i(\vec{k}) d\vec{k} + F[\rho(\vec{r})] \tag{15}$$

where the first term is a sum over the self-consistent eigenvalues, and the second term, a functional of the charge density, contains all non-band structure contributions to the energy. In non self-consistent calculations, the band structure now contains an arbitrary zero which must be fixed in order to calculate the total energy. The arbitrariness of the energy zero in the tight binding method can be exploited to recast the total energy as

$$E = \int \sum_i \varepsilon_i'(\vec{k}) d\vec{k} \tag{16}$$

where the new eigenvalues are shifted in energy such that $\varepsilon_i' = \varepsilon_i - F[\rho(\vec{r})]$. With this formulation, the total energy is given simply as a sum over the bands, eliminating the need for pair potential repulsive terms which are often included in other treatments. The parameters of the tight binding model are determined by fitting to accurate LAPW band structures and total energies. This approach has been very successful in describing the properties of a wide variety of monatomic systems such as iron, silicon, and xenon (Cohen et al. 1997b). The approach can be generalized to multicomponent systems including silicates but this has not yet been accomplished.

Semi-empirical atomistic models

The primary advantage of these highly approximate methods is that they are computationally fast, allowing one to examine much larger systems, or more complex physics than one could otherwise. In most cases they revert to our more traditional view of solids as being composed of ions rather than nuclei and electrons; the latter generally do not appear explicitly. This strictly precludes these methods from the study of systems in which electronic effects are important, such as those in which electronic (e.g. insulator-metal) transitions occur or in which magnetism is relevant. The atomistic picture also limits the transferability of semi-empirical models to a more or less narrow range of compounds or structures over which the bonding does not change substantially. Within the range of transferability, semi-empirical potentials may be made to fit experimental data with some accuracy and can lead to useful predictions of material behavior under conditions that have not yet been accessed experimentally, of previously unobserved behavior, or of similar materials.

Many of these models can be cast in the following form

$$E = \sum_{i<j} V_2(r_{ij}) + \sum_{i<j<k} V_3(r_{ij}, r_{ik}, r_{jk}) + \ldots \quad (17)$$

where E is the total energy of an atomic configuration, the sums are over the atoms in the system, and V_2 and V_3 are two-body (pair) and three-body potentials respectively. Higher order terms can be included although the sum may not converge rapidly for many systems. This approach is appealing in the case of ionic materials such as oxides and silicates because the largest part of the energy is the Madelung term, a sum of pair-wise interactions. The simplest semi-empirical model of an ionic solid consists of the Madelung term and pair-wise short-range repulsive forces. This widely studied model was originally applied to simple systems such as alkali halides but has more recently been used to investigate the behavior of oxides and silicates (Burnham 1990). However, short-range attractive and repulsive interactions, though energetically secondary, can strongly influence the structure and other properties of the system. These forces are often substantially more complex than the Coulomb potential and may require elaborate and non-unique functional forms and/or three-body or even higher-order terms for accurate representation.

DERIVATION OF OBSERVABLES

Total energy and band structure

For a given arrangement of nuclei (crystal structure) we may use any of the above methods to determine the total energy. First-principles and ab initio methods also yield the charge density, and the quasi-particle eigenvalue spectrum (electronic band structure). By examining the dependence of the total energy on perturbations to the volume V or shape of the crystal (described by the deviatoric strain tensor ε_{ij}) or to the positions of the atoms, the Helmholtz free energy F as a function of V, ε_{ij}, and temperature T can in principle be deduced. For example, the static pressure and the equation of state are simply given by the variation of the total energy with volume.

One may determine the elastic constants from total energy calculations. For small deviatoric strains under hydrostatic stress (Wallace 1972)

$$F(V, \varepsilon'_{ij}, T) = F_0(V) + F_{TH}(V, T) + \frac{1}{2} c_{ijkl}(V, T) \varepsilon'_{ij} \varepsilon'_{kl} \quad (18)$$

where F_0 is the static (zero temperature) contribution, F_{TH} is due to the thermal excitation of electrons and phonons, and c_{ijkl} is the elastic constant tensor. This equation shows that combinations of elastic constants are related to the difference in total energy between a strained and unstrained lattice.

It is possible in principle to calculate thermal contributions to the thermodynamic and thermoelastic properties of crystals. Calculating thermal properties is much more difficult than calculating static properties, however. The reason is simple: the atomic vibrations induced by finite temperature break the symmetry of the crystal so that it is now periodic only in a time averaged sense. In the context of total energy calculations, our task is then to evaluate the partition function, an integral over all atomic configurations realized by a crystal at high temperature. While this is not difficult with semi-empirical or ab initio models, it is still essentially impossible with first-principles methods for most systems. More efficient ways of evaluating thermal free energies from first principles are required. Some future directions are indicated in the penultimate section.

Forces, stresses, and structures

The Hellman-Feynman theorem allows one to calculate first derivatives of the total

energy directly in terms of the ground
allows one to determine the forces a
lattice.

This is important for two related
crystal structures very effectively. In f
only recently for relatively complex st
al. 1993). The key innovation has
strategy based on a pseudo-Lagrangia
the atomic positions as dynamical v
performed at constant pressure. At e
Feynman forces and stresses (Nielsen
and lattice parameters are evaluated
optimization is complete when the for
and balances the applied pressure.

Second, once the ground state s
calculate the static elastic constants. T
deviatoric strain to the lattice and
constant, c_{ijkl} is then given by the ratio

$$\sigma_{ij} = c_{ijkl} \varepsilon_{kl}$$

Care must be taken to re-optimize the
since vibrational modes typically c
addition, the elastic moduli under pr
defined in several ways; and attention

Linear response

This approach goes one step be
changes in the total energy to second
order changes in the charge densit
perturbations may include the displa
field. The wavelength of the perturb
allowing one to investigate, for instan
tremendous computational and concep

In the context of mineralogy, the
related to second-derivatives of the to
elements of the dynamical matrix, t
charge tensor. With these quantiti
throughout the Brillouin zone (Lee a
making contact with experimental obs
predictions allow one to investigate pl
are quasiharmonic, high temperature
subtle and necessarily involves not o
the dielectric constant and Born effect
field at zone-center is properly accoun

C

Methods

First-principles methods based
expanding the wavefunctions in a bas

energy directly in terms of the ground state wavefunctions. The application of this theorem allows one to determine the forces acting on every atom and the stresses acting on the lattice.

This is important for two related reasons. First, it allows one to determine ground state crystal structures very effectively. In first principles calculations, this has become possible only recently for relatively complex structures such as $MgSiO_3$ perovskite (Wentzcovitch et al. 1993). The key innovation has been the development of a structural optimization strategy based on a pseudo-Lagrangian that treats the components of the strain tensor and the atomic positions as dynamical variables (Wentzcovitch 1991). The optimization is performed at constant pressure. At each step of the dynamical trajectory, the Hellman-Feynman forces and stresses (Nielsen and Martin 1985) acting, respectively, on the nuclei and lattice parameters are evaluated and used to generate the next configuration. The optimization is complete when the forces on the nuclei vanish and the stress is hydrostatic and balances the applied pressure.

Second, once the ground state structure at a given pressure is determined, one can calculate the static elastic constants. This is done in a straightforward way by applying a deviatoric strain to the lattice and calculating the resulting stress tensor. The elastic constant, c_{ijkl} is then given by the ratio of stress σ_{ij} to strain ε_{ij}

$$\sigma_{ij} = c_{ijkl}\varepsilon_{kl} \tag{19}$$

Care must be taken to re-optimize the positions of the atoms in each strained configuration since vibrational modes typically couple with lattice strains in silicate structures. In addition, the elastic moduli under pressure (so-called effective elastic constants) may be defined in several ways; and attention must be given to the correct definition.

Linear response

This approach goes one step beyond the Hellman-Feynman theorem by computing changes in the total energy to second order. This is accomplished by computing the first order changes in the charge density in response to generalized perturbations. These perturbations may include the displacement of an atom, or the application of an electric field. The wavelength of the perturbation need not be commensurate with the unit cell, allowing one to investigate, for instance, phonon modes without resorting to supercells, a tremendous computational and conceptual advantage (Baroni et al. 1987).

In the context of mineralogy, the advantage of this approach is that properties that are related to second-derivatives of the total energy can be computed directly. Examples include elements of the dynamical matrix, the dielectric constant tensor and the Born effective charge tensor. With these quantities, the full phonon spectrum can be determined throughout the Brillouin zone (Lee and Gonze 1995, Stixrude et al. 1996). In addition to making contact with experimental observation of zone-center vibrational frequencies, these predictions allow one to investigate phase stability, and, to the extent that thermal properties are quasiharmonic, high temperature properties. The computation in polar substances is subtle and necessarily involves not only the calculation of force constants, but also that of the dielectric constant and Born effective charge tensors so that coupling to the macroscopic field at zone-center is properly accounted for (LO-TO splitting).

COMPUTATION

Methods

First-principles methods based on density functional theory solve Equations (6-8) by expanding the wavefunctions in a basis

$$\psi_i(\vec{r},\vec{k}) = \sum_{j=1}^{N} c_{ij}\phi_j(\vec{r},\vec{k}) \qquad (20)$$

where N is the number of basis functions, ϕ_j and c_{ij} are the coefficients to be determined by solution of the Kohn-Sham equations.

The LAPW method is the current state-of-the-art in density functional theory computations. It makes no essential approximations beyond that to the exchange-correlation functional, allowing one to routinely solve for all electrons, core and valence. For example, it makes no approximations to the shape of the charge density or potential. The accurate representation of the potential and the core states means that the LAPW method is equally applicable to all elements of the periodic table, and over the entire range of densities of interest in planetary or astrophysical studies.

The LAPW differs from its forerunner, the APW method, in that in practical application, APW assumes a constant potential between the muffin-tin spheres that surround each nucleus (Bukowinski 1977, 1985). Because of its precise representation of the potential, the LAPW method is sometimes referred to as FLAPW, for "full-potential". LAPW shares the ability to precisely represent the full potential and charge density with the full-potential LMTO method (Söderlind et al. 1996). The FP-LMTO method is very similar to LAPW in its capabilities and level of accuracy, differing primarily in the details of the basis functions.

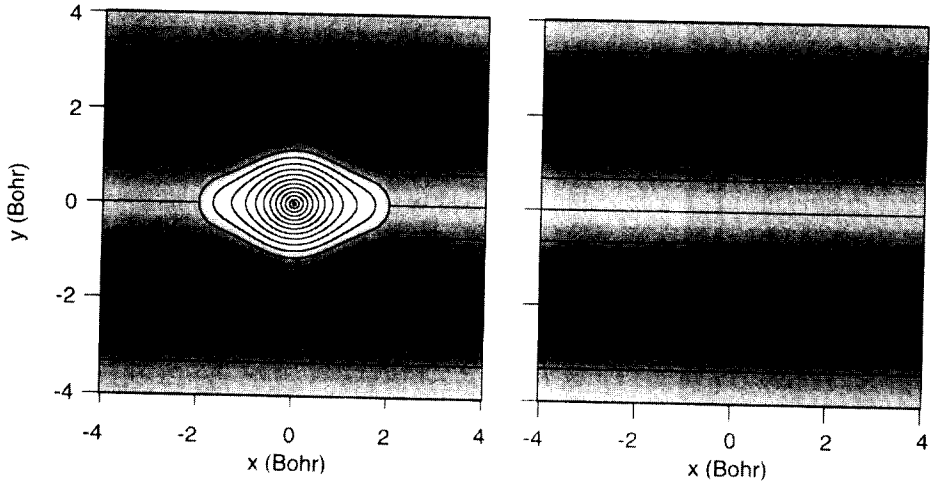

Figure 4. Left: A single LAPW basis function in the vicinity of a hydrogen nucleus located at the origin: $k = 0$, $\vec{G} = (0, \pi/2, 0)$, $l_{max} = 6$, $E_l(\mathrm{Ry}) = -(l+1)^2$. Right: The plane wave $\vec{G} = (0, \pi/2, 0)$.

The accuracy and flexibility of the LAPW method derives from its basis which explicitly treats the first-order partitioning of space into near-nucleus regions, where the charge density and its spatial variability are large, and interstitial regions, where the charge density varies more slowly (Fig. 4) (Anderson 1975, Singh 1994, Wei and Krakauer 1985). These two regions are delimited by the construction of so-called muffin-tin spheres of radius R_{MT}^{α} centered on each nucleus α. A dual-basis set is constructed, consisting of plane-waves in the interstitial regions that are matched continuously to more rapidly varying functions inside the spheres. Within the muffin-tin spheres $r' < R_{MT}^{\alpha}$

$$\phi^{\vec{k}+\vec{G}}(\vec{r}) = \left[a_{lm}^{\alpha} u_l(E_l^{\alpha}, r') + b_{lm}^{\alpha}\right.$$

and for $r' > R_{MT}^{\alpha}$

$$\phi^{\vec{k}+\vec{G}}(\vec{r}) = exp\left[i\left(\vec{k}+\vec{G}\right)\bullet\vec{r}\right]$$

where $\vec{r}' = \vec{r} - \vec{R}_{\alpha}$, $\vec{R}_{\alpha}$ are the position reciprocal lattice vector, u_l and $\dot{u}_l$ ar Schrödinger equation and its energy d potential inside the muffin-tin sphe determined by requiring continuity of muffin-tin sphere.

With this basis set, all-electron require on the order of 100 basis f LAPW method is that the complexity computationally. In practice, this limi LAPW computations for structures a the unit cell) have been performed (S

Basis sets consisting solely of pl significant advantages over the LA virtually impossible with a plane wa represent the rapid spatial oscillation For this reason, the plane wave basis approximation, in which the Fourier design.

Convergence

There are two primary converge over reciprocal space (e.g. Eqn. 9) property of smooth convergence; t readily assessed; quantities of interes the LAPW method, the size of the $R_{MT}K_{max}$, where K_{max} is the maxim basis set. In the pseudopotential meth energy of the plane waves $E_{cut} = K_{ma}$ silicates are $R_{MT}K_{max} = 7$ and $E_{cut} =$ used.

Sampling of the Brillouin zone been shown to yield rapid convergen few points (1-10) are typically nee require denser sampling because of special points method constructs a u first Brillouin zone. The resulting symmetrically equivalent points. T member of each star, and the wavef the appropriate symmetry operatio degeneracy.

$$\phi^{\vec{k}+\vec{G}}(\vec{r}) = \left[a_{lm}^{\alpha} u_l(E_l^{\alpha}, r') + b_{lm}^{\alpha} \dot{u}_l(E_l^{\alpha}, r')\right] Y_{lm}(\vec{r}/r) \quad (21)$$

and for $r' > R_{MT}^{\alpha}$

$$\phi^{\vec{k}+\vec{G}}(\vec{r}) = exp\left[i\left(\vec{k}+\vec{G}\right) \bullet \vec{r}\right] \quad (22)$$

where $\vec{r}' = \vec{r} - \vec{R}_{\alpha}$, $\vec{R}_{\alpha}$ are the positions of the nuclei, $\vec{k}$ is in the first Brillouin zone, $\vec{G}$ is a reciprocal lattice vector, u_l and $\dot{u}_l$ are, respectively, the solution to the radial part of the Schrödinger equation and its energy derivative for the spherically symmetric portion of the potential inside the muffin-tin sphere at energy E_l, and the coefficients a and b are determined by requiring continuity of the basis function and its first radial derivative on the muffin-tin sphere.

With this basis set, all-electron calculations for silicates or transition metals typically require on the order of 100 basis functions per atom. The primary disadvantage of the LAPW method is that the complexity of the basis functions makes it relatively intensive computationally. In practice, this limits the size of the system that can be studied. Even so, LAPW computations for structures as complex as that of $MgSiO_3$ perovskite (20 atoms in the unit cell) have been performed (Stixrude and Cohen 1993).

Basis sets consisting solely of plane waves, because of their analytical simplicity have significant advantages over the LAPW basis. However, all-electron calculations are virtually impossible with a plane wave basis set; the number of basis functions needed to represent the rapid spatial oscillations of the core region is much too large to be practical. For this reason, the plane wave basis is generally linked in practice to the pseudopotential approximation, in which the Fourier content of charge density and potential are limited by design.

Convergence

There are two primary convergence issues: the size of the basis, and the integrations over reciprocal space (e.g. Eqn. 9). Both LAPW and plane-wave basis sets have the property of smooth convergence; this means that convergence of the computations is readily assessed; quantities of interest vary smoothly as the basis set size is increased. In the LAPW method, the size of the basis set is described by the dimensionless quantity $R_{MT}K_{max}$, where K_{max} is the maximum wavenumber of the plane waves included in the basis set. In the pseudopotential method, the size of the basis is set by the maximum kinetic energy of the plane waves $E_{cut} = K_{max}^2$ in atomic units. Typical values for computations of silicates are $R_{MT}K_{max} = 7$ and $E_{cut} = 40$-80 Ry, depending on the pseudopotential that is used.

Sampling of the Brillouin zone is treated with the special points method, which has been shown to yield rapid convergence (Monkhurst and Pack 1976). For insulators, only a few points (1-10) are typically needed to achieve fully converged total energies; metals require denser sampling because of the often complex structure of the Fermi surface. The special points method constructs a uniform grid of k-points of specified resolution in the first Brillouin zone. The resulting set of k-points is divided into subgroups (stars) of symmetrically equivalent points. The Kohn-Sham equations are solved for only one member of each star, and the wavefunctions at other points in the star reconstructed with the appropriate symmetry operations, weighting the contribution of each star by its degeneracy.

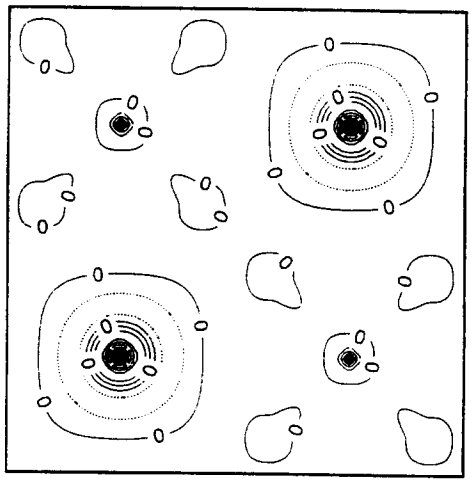

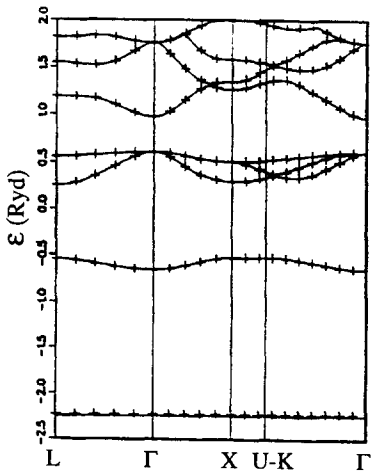

Figure 5 (left). Difference in charge density of MgO generated with overlapping ions using a Gordon-Kim model (potential-induced breathing, or PIB model) (Isaak et al. 1990) and calculated self-consistently using the linearized augmented plane wave (LAPW) method (Mehl et al. 1988). Contour interval: 0.005 e/Bohr^3 (see also Hemley and Cohen 1996).

Figure 6 (right). Band structure of MgO near zero pressure calculated using the LAPW method (lines) compared with that determined from the potential generated by the overlapping ion PIB charge density (Isaak et al. 1990, Mehl et al. 1988).

SELECTED APPLICATIONS

Bonding and electronic structure

Ab initio models give insight into bonding and electronic structure that are often not obvious from self-consistent computations alone. One example is the relationship among and meaning of ionicity, covalency, and band width. One might think for example that a purely ionic model would have atomic-like energy levels, and that band width would arise from hybridization or covalency. Figure 5 shows the difference in charge density of MgO computed with overlapping PIB ions and computed self-consistently using the LAPW method. The agreement is excellent. Furthermore, the bands that one finds using the crystal potential computed from the PIB charge density are in excellent agreement with the self-consistent band structure (Fig. 6). Thus, the PIB charge density is a good approximation to the self-consistent charge density for ionic materials such as MgO. A similar comparison should be made for rare-gas solids.

Thus, bands computed from the potential generated from overlapping ionic charge densities not only have width, but are in excellent agreement with self-consistent computations for ionic crystals. If one were to ask the origin of the band width in a tight-binding representation, one would find that the O $2p$ band width in MgO, for example, comes primarily from O-O $pp\sigma$ interactions (Kohan and Ceder 1996). We see that even a purely ionic charge density, generated by overlapping spherical ions, has a charge density that generates a potential, that when used in the KS equations implies a band width consistent with hybrid electronic states. There is a sort of duality in the description of ionic materials in that they can also be described from a charge density or tight-binding (or LCAO) perspective. In either case, there must be long-range Madelung terms in the total energy, that gives rise to LO-TO splitting in the lattice dynamics.

Not all ionic solids are formed f
solid solutions between MgO and Fe
is a d_6 ion and is not closed shell.
insulators, which are discussed
theoretically, and in spite of the in
method for obtaining first-principles
models such as PIB fail to give ac
properties for these materials, ev
Nevertheless, much can be learned a
as described below. Perhaps simpl
these materials, but it has not yet bee

Figure 7. The equation of state of three different polytypes of $MgSiO_3$ perovskite as determined by LAPW calculations in the LDA approximation (Stixrude and Cohen 1993). The *Pbnm* structure is found to be most stable throughout the pressure regime of the earth's mantle. This is in agreement with experimental observations which so far have found no reproducible observations of other stable aristotypes. Circles and squares are experimental data from (Knittle and Jeanloz 1987) and (Mao et al. 1991), respectively.

Pressure (GPa)

Equation of state

The error due to the LDA in firs
the results of LAPW calculations, w
the LDA, with experiment (Fig. 7).
found that errors in volumes are ty
smaller than experimental (Cohen
1993). Part of this small difference
K) compared with the athermal calc
for a theory which is parameter free

All electron LDA computations
in the zero pressure volume; for
underestimate the experimental vol
complex (Sigalas et al. 1992). For
orbit coupling, often neglected in c
the discrepancy between theory an
improves the agreement between
materials including the 3d transitio

Not all ionic solids are formed from closed shell ions. For example, FeO (wüstite) and solid solutions between MgO and FeO (magnesiowüstite) behave like ionic solids, yet Fe^{2+} is a d_6 ion and is not closed shell. FeO belongs to a class of materials known as Mott insulators, which are discussed below. Such materials are very difficult to treat theoretically, and in spite of the importance of Fe in minerals, there is not yet a good method for obtaining first-principles results that are completely correct. Moreover, ab initio models such as PIB fail to give accurate predictions for the equation of state and other properties for these materials, even if one sphericalizes Fe, and treats it as ionic. Nevertheless, much can be learned about these materials from self-consistent computations as described below. Perhaps simple and accurate ab initio models can be developed for these materials, but it has not yet been done.

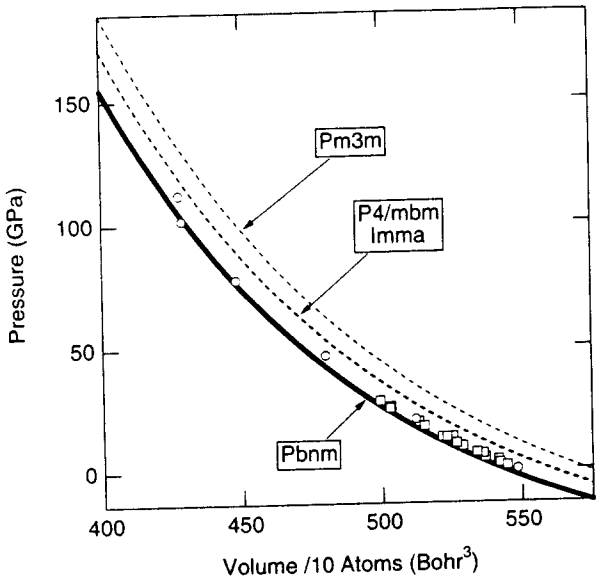

Figure 7. The equation of state of three different polytypes of $MgSiO_3$ perovskite as determined by LAPW calculations in the LDA approximation (Stixrude and Cohen 1993). The *Pbnm* structure is found to be most stable throughout the pressure regime of the earth's mantle. This is in agreement with experimental observations which so far have found no reproducible observations of other stable aristotypes. Circles and squares are experimental data from (Knittle and Jeanloz 1987) and (Mao et al. 1991), respectively.

Equation of state

The error due to the LDA in first principles calculations can be evaluated by comparing the results of LAPW calculations, which make no further essential approximations beyond the LDA, with experiment (Fig. 7). In investigations of silicates and oxides, it has been found that errors in volumes are typically 1-4% with theoretical volumes being uniformly smaller than experimental (Cohen 1991, 1992; Mehl et al. 1988, Stixrude and Cohen 1993). Part of this small difference is due to the higher temperatures of experiments (300 K) compared with the athermal calculations. This is a highly satisfactory level of agreement for a theory which is parameter free and independent of experiment.

All electron LDA computations of transition metals show errors of similar magnitude in the zero pressure volume; for the 3d and 4d metals, the calculations uniformly underestimate the experimental volumes, while for the 5d metals, the situation is more complex (Sigalas et al. 1992). For the heaviest materials, additional effects such as spin-orbit coupling, often neglected in computations, may become important and contribute to the discrepancy between theory and experiment. The generalized gradient approximation improves the agreement between theory and experimental equations of state for most materials including the 3d transition metals. In the case of iron, LAPW and FP-LMTO

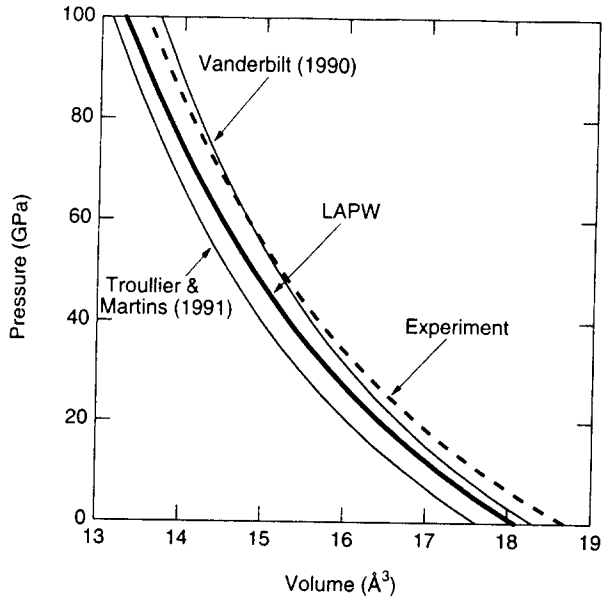

Figure 8. Equation of state of MgO from (dashed line) experiment (Duffy et al. 1995), (bold line) all-electron LDA (LAPW) calculations, (thin lines) pseudopotential calculations based on the indicated potentials (Troullier and Martins 1991, Vanderbilt 1990).

calculations differ from the experimentally measured room temperature equation of state by 3 % at zero pressure and by less than 1 % at core pressures (Sherman 1997, Söderlind et al. 1996, Stixrude et al. 1994); agreement with high temperature Hugoniot data is equally good (Stixrude et al. 1997).

Pseudopotential calculations make additional approximations that lead to additional errors (Fig. 8). These are small in magnitude and comparable in size to the LDA error. At this level of detail, different pseudopotentials yield results that differ from each other and from the all-electron LDA result from LAPW. Because the pseudopotential method is nearly as accurate as the much more elaborate LAPW method, it is often preferred for many applications, since its computational advantages allow much larger, and more complex systems to be studied.

Structure and compression mechanisms

The structure and compression mechanisms of a number of complex silicates have been studied with density functional theory at high pressure, including $MgSiO_3$ enstatite and perovskite, Mg_2SiO_4 forsterite, ringwoodite and inverse ringwoodite, and SiO_2 in the quartz, stishovite, $CaCl_2$ and columbite structures (Cohen 1991, 1992; Karki et al. 1997a, Karki et al. 1997d, Kiefer et al. 1998, Wentzcovitch et al. 1995a, Wentzcovitch et al. 1993, Wentzcovitch et al. 1995b, Wentzcovitch et al. 1998, Wentzcovitch and Stixrude 1997). Although simple ab initio models provide important predictions for high-pressure behavior of many deep earth materials, such as $MgSiO_3$ perovskite (Hemley et al. 1987, Cohen 1987b, Wolf and Bukowinski 1987), the need for an extended treatment relative to such simple approaches is readily seen: for example in the case of MgSiO,: the density, crystal structure parameters, and elasticity cannot all be explained from standard ionic models (i.e. assuming full charges on the ions) (Hemley and Cohen 1992). These investigations (1) provide an important test of the approximations upon which first-principles methods are based (2) illustrate in detail often not obtainable by experiment the nature of compression mechanisms and (3) provide a sensitive test of the hypothesis that

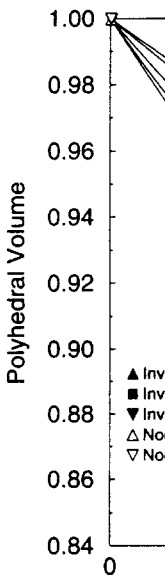

Figure 9. Compression of coordination
pseudopotential calculations (Kiefer et al

some minerals undergo high-order

Using the method of Wentzc
the first principles optimization
efficient procedure. Typically, o
structural convergence in this min
parameters (Wentzcovitch and Sti
first principles calculations show
taken up by the MgO_6 octahedra w
the inverse form, the MgO_4 tetrah
than the MgO_6 octahedra in the no
that, in the inverse structure, Si
octahedral layers, leaving most of
1998).

Phase stability

In many ways, phase stabil
methods. The reason is that we a
structures, with different basis
transformations, generally a minu
million).

First principles LDA total ene
have shown excellent agreement
Karki et al. 1997b,d; Kingma et
include the prediction, based on I

Figure 8. Equation of state of MgO from (dashed line) experiment (Duffy et al. 1995), (bold line) all-electron LDA (LAPW) calculations, (thin lines) pseudopotential calculations based on the indicated potentials (Troullier and Martins 1991, Vanderbilt 1990).

rature equation of state by herman 1997, Söderlind et e Hugoniot data is equally

ns that lead to additional size to the LDA error. At liffer from each other and seudopotential method is s often preferred for many rger, and more complex

f complex silicates have cluding $MgSiO_3$ enstatite woodite, and SiO_2 in the 1992; Karki et al. 1997a, 95a, Wentzcovitch et al. entzcovitch and Stixrude ictions for high-pressure te (Hemley et al. 1987, nded treatment relative to of $MgSiO_3$: the density, ned from standard ionic d Cohen 1992). These ions upon which first- inable by experiment the of the hypothesis that

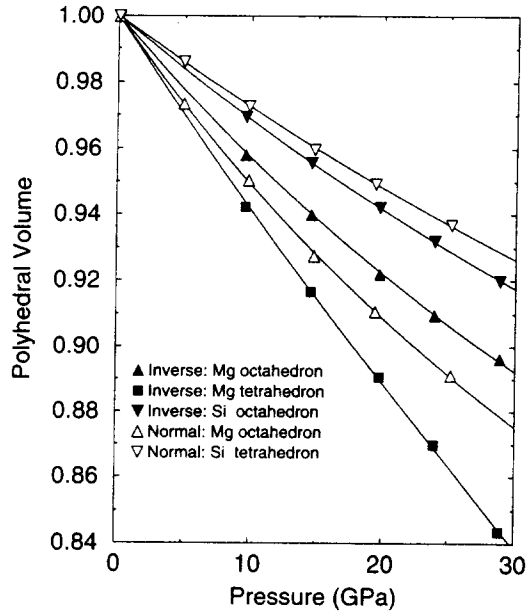

Figure 9. Compression of coordination polyhedra in normal and inverse Mg_2SiO_4 ringwoodite from LDA pseudopotential calculations (Kiefer et al. 1998).

some minerals undergo high-order symmetry-invariant phase transformations.

Using the method of Wentzcovitch (Wentzcovitch 1991, Wentzcovitch et al. 1993), the first principles optimization of complex crystal structures such as forsterite is an efficient procedure. Typically, on the order of 10-20 iterations are required for full structural convergence in this mineral with 7 internal degrees of freedom and three lattice parameters (Wentzcovitch and Stixrude 1997). In the case of ringwoodite, the results of first principles calculations show that, in the normal form, volume compression is mostly taken up by the MgO_6 octahedra which are much softer than the SiO_4 tetrahedra (Fig. 9). In the inverse form, the MgO_4 tetrahedra are the most compressible polyhedra, softer even than the MgO_6 octahedra in the normal form. This result can be understood by recognizing that, in the inverse structure, Si- and Mg-polyhedra combine to form relatively rigid octahedral layers, leaving most of the compression to the tetrahedral layers (Kiefer et al. 1998).

Phase stability

In many ways, phase stability provides the most stringent test of first-principles methods. The reason is that we are comparing total energies computed for two different structures, with different basis sets and Brillouin zones at the level of heats of transformations, generally a minuscule fraction of the total energy (less than one part per million).

First principles LDA total energy calculations of transformations in oxides and silicates have shown excellent agreement with experiment (Cohen 1991, 1992; Isaak et al. 1993, Karki et al. 1997b,d; Kingma et al. 1996, Mehl et al. 1988, Teter et al. 1998). These include the prediction, based on LAPW calculations, of the stishovite to $CaCl_2$ transition

(Cohen 1991, 1992) which was later found and confirmed experimentally (Kingma et al. 1995). Subsequent pseudopotential calculations are in excellent agreement with the earlier LAPW results showing that careful calculations yield consistent results even though computational methods may be quite different (Figs. 10 and 11). There is considerable interest in the possibility of still higher pressure phases that may be stable deep within the lower mantle. First principles calculations predict a phase transition near 96 GPa from the $CaCl_2$ structure to the columbite (α-PbO_2) structure (Karki et al. 1997d,e). This ultrahigh

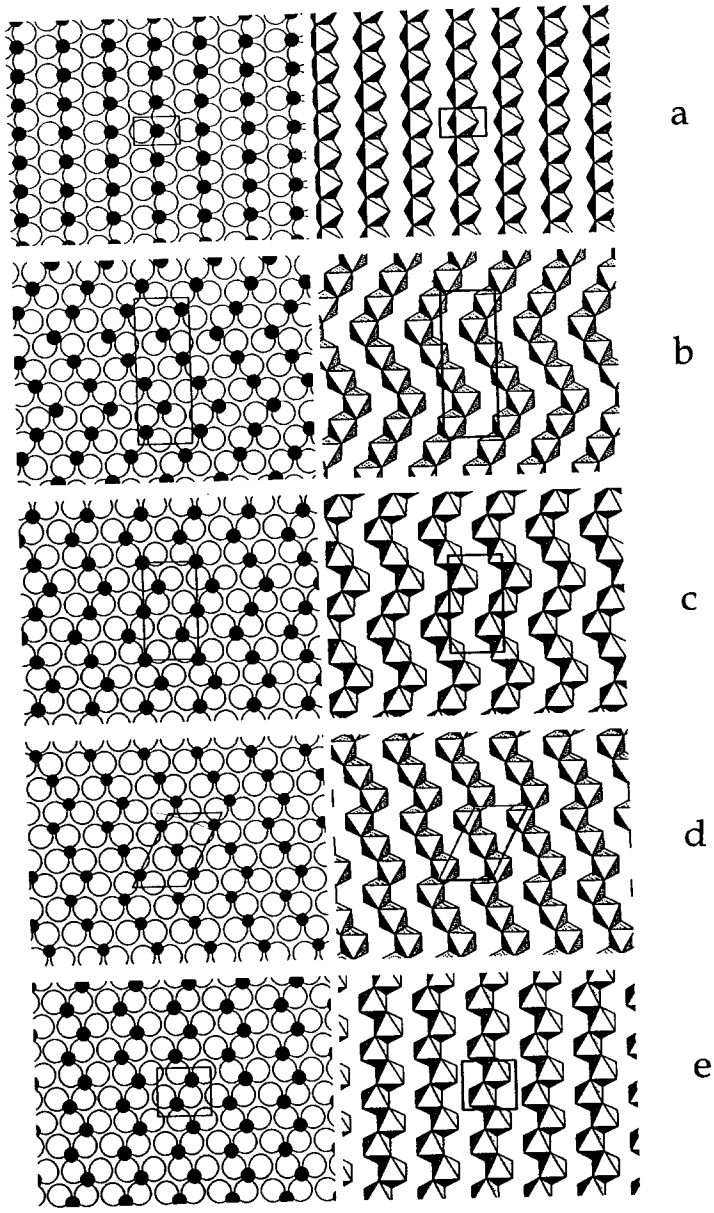

Figure 10. Opposite page: Representat
1998). (a) $CaCl_2$, (b) SnO_2 (4 × 4) (c) NaTiF
left-hand figures show one layer of the *ABA*
the octahedral interstices filled with silicon
form edge-sharing octahedral chains with var

Below, right: Enthalpies of the structures relative to that of stishovite as a function of pressure.

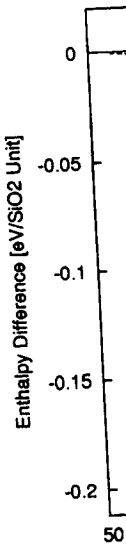

pressure structure is built of S
polymorphs primarily in the kinki
that there is a large number of clos
stable at pressures above 50 GPa
close packing of the oxygen anion
calculations predict that the colum
the calculations of Karki et al. (19
phases with similar bonding top
experimentally (Hemley et al. 199

In the case of transition m
critical. LDA fails to predict the c
phase has a lower total energy th
state. Moreover, it accurately pre
near 11 GPa (Stixrude et al. 199
particularly subtle in the case of t
magnetic phase. These calculatio
phase of iron at pressures beyon
al. 1990). First principles calcula
as a stable phase at extreme pre
exchange-correlation potential.
instability with respect to a tetra
150 GPa, the bcc structure wi
inner core is likely composed of
or nearly hexagonal phase, or fc

Figure 10. Opposite page: Representations of dense silica structures calculated by LDA (Teter et al. 1998). (a) $CaCl_2$, (b) SnO_2 (4 × 4) (c) $NaTiF_4$ (3 × 3), (d) $P2_1/c$ (3 × 2), and (1) a-PbO_2 structure types. The left-hand figures show one layer of the *ABAB* ... ... stacking of hcp oxygen anions (white) with one-half of the octahedral interstices filled with silicon ions (black). The right-hand figures show how these patterns form edge-sharing octahedral chains with various degrees of kinking (given in parentheses above).

Below, right: Enthalpies of the structures relative to that of stishovite as a function of pressure.

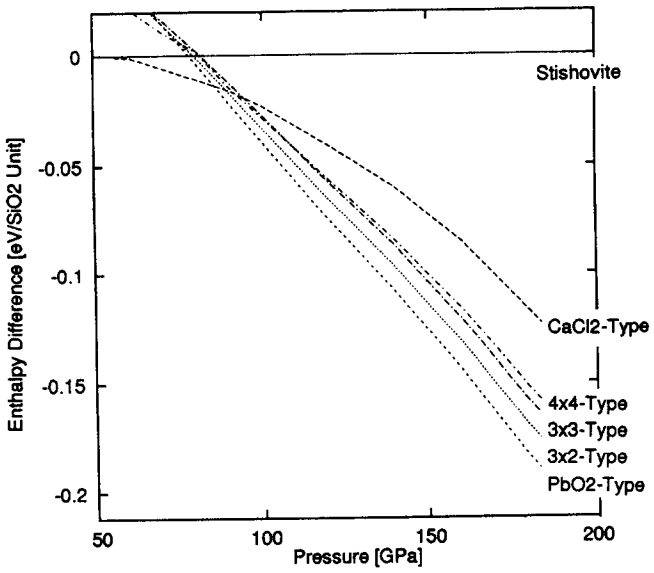

pressure structure is built of SiO_6 octahedra and differs from the lower pressure polymorphs primarily in the kinking of the chains of octahedra. Teter et al. (1998) found that there is a large number of closely related, and energetically competitive phases that are stable at pressures above 50 GPa (Fig. 10). These structures are all based on essentially close packing of the oxygen anions with different ordering of Si in the octahedral sites. The calculations predict that the columbite structure is stable above 80 GPa, in agreement with the calculations of Karki et al. (1997d,e), but that there should be extensive metastability of phases with similar bonding topology at these pressures; this appears to be observed experimentally (Hemley et al. 1994, Teter et al. 1998).

In the case of transition metals, the form of the exchange-correlation potential is critical. LDA fails to predict the correct ground state of iron, finding incorrectly that the hcp phase has a lower total energy than the bcc. The GGA correctly recovers the bcc ground state. Moreover, it accurately predicts the pressure of the phase transition from bcc to hcp near 11 GPa (Stixrude et al. 1994). This is an important result because the energetics are particularly subtle in the case of this transition since it involves a ferromagnetic and a non-magnetic phase. These calculations find that the hcp phase is the stable low temperature phase of iron at pressures beyond 11 GPa, in excellent agreement with experiment (Mao et al. 1990). First principles calculations show that it is highly unlikely that bcc will reappear as a stable phase at extreme pressures and temperatures, independent of the form of the exchange-correlation potential. The reason is that bcc is found to undergo an elastic instability with respect to a tetragonal strain at high pressure (Fig. 12). At pressures beyond 150 GPa, the bcc structure will spontaneously distort (Stixrude and Cohen 1995). The inner core is likely composed of a close-packed structure, either hcp or a similar hexagonal or nearly hexagonal phase, or fcc.

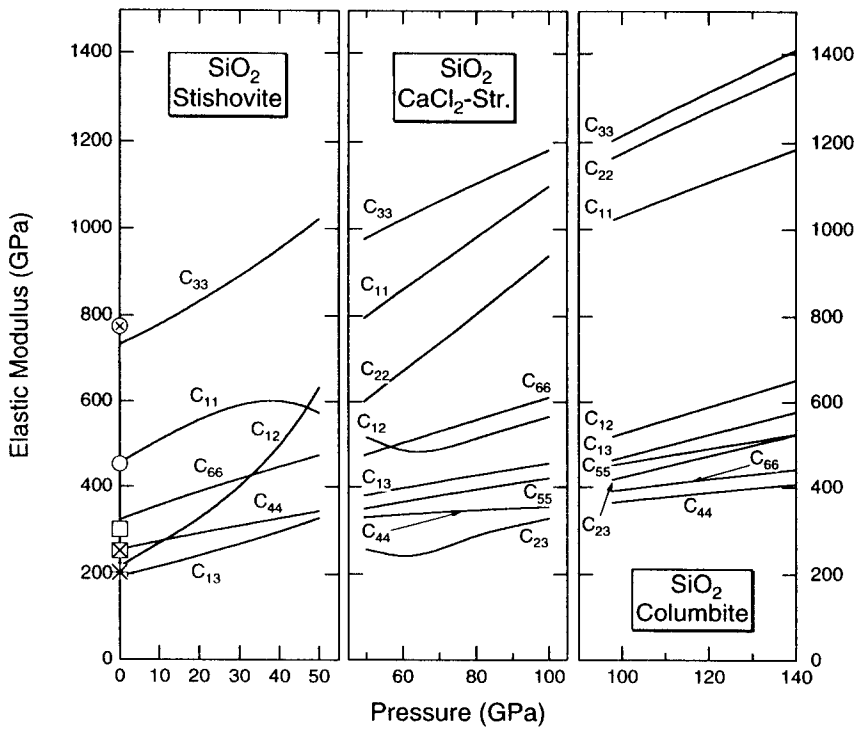

Figure 11. Elastic constants of three high-pressure phases of silica from LDA pseudopotential calculations (Karki et al. 1997c). The pressure of the phase transition from stishovite to the $CaCl_2$ structure is in excellent agreement with experiment (Kingma et al. 1995); while the predicted phase transition to the columbite structure is consistent with some of the diffraction data reported by Kingma et al. (1996) (see also Teter et al. 1998). Experimentally measured elastic constants of stishovite are indicated by the symbols (Weidner et al. 1982).

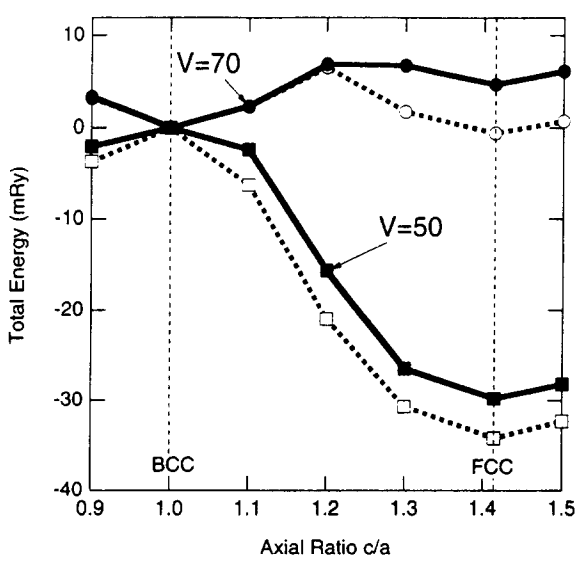

Figure 12. First principles LAPW calculations of the energy vs. *c/a* ratio of iron within GGA (solid curves) and LDA (dashed) approximations at two volumes: 70 $Bohr^3$ (~10 GPa, upper curves) and 50 $Bohr^3$ (~200 GPa, lower curves). The *c/a* ratios of the bcc and fcc structures are indicated. The change in the curvature of the energy surface at bcc is an elastic instability (Stixrude et al. 1994).

Another approach towards phase s
lattices. One example of this approa
response computations with the
perovskite structure (Fig. 13). U
studies have found $CaSiO_3$ to be cu
in the theoretical calculations to be
boundary. The unstable vibrational
which lower the symmetry. Frozer
suggest strongly that $CaSiO_3$ is n
strain predicted theoretically is con
were interpreted as showing a cubi

Ab initio models can also be
search for possible phase transitior
model showed a high pressure elas
for different structures showed a pl
(Cynn et al. 1990), and the trans
using the LAPW method with the
Pseudopotential calculations are
computations predicted a phase tra
experiments (Funamori and Jean
further transition to a perovskite pl
(i.e. at 223 GPa).

Elastic moduli

The elastic moduli are of centr
govern the passage of seismic wav
the subsurface. Despite their im
constants of earth materials have
that of an efficient structural o
calculation of stresses from th
determined by calculating the
equilibrium structure as described
within the linear regime by perfor
magnitude and extrapolating to
calculations show that strains of t
By carefully choosing the symm
elements of the elastic constant
example, the three elastic consta
strain; four different strains have
elastic constants) (Silva et al. 199

The full elastic constant tensors c
with the plane-wave pseudopoter
perovskite, Mg_2SiO_4 forsterite a
columbite structures (Karki et
Wentzcovitch et al. 1993). O
straightforward to calculate the ela
anisotropy, and the seismic-wave
11) show several interesting featu
structure is associated with an ela
octahedral rotation and basal pla

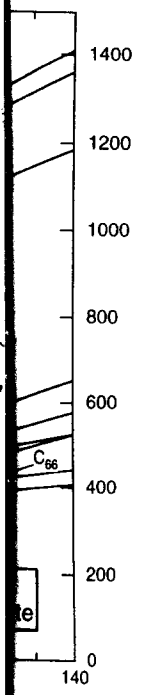

A pseudopotential
the $CaCl_2$ structure
se transition to the
et al. (1996) (see
ted by the symbols

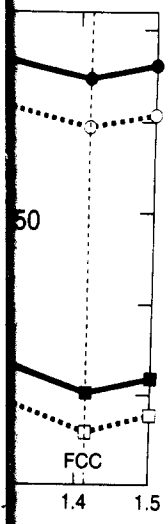

Another approach towards phase stability is the investigation of the dynamical stability of lattices. One example of this approach is that of Stixrude et al. (1996) who performed linear response computations with the LAPW method on $CaSiO_3$ perovskite in the cubic perovskite structure (Fig. 13). Unlike $MgSiO_3$, which is orthorhombic, experimental studies have found $CaSiO_3$ to be cubic. Unexpectedly, however, cubic $CaSiO_3$ was found in the theoretical calculations to be unstable at the *M*- and *R*- points on the Brillouin zone boundary. The unstable vibrational modes correspond to rotations of the SiO_6 octahedra which lower the symmetry. Frozen phonon calculations confirmed this result. The results suggest strongly that $CaSiO_3$ is not cubic but tetragonal or lower symmetry. The small strain predicted theoretically is consistent with the expected precision of x-ray studies that were interpreted as showing a cubic structure for $CaSiO_3$.

Ab initio models can also be used to study the stability of a variety of structures to search for possible phase transitions. This was done successfully for Al_2O_3, where the PIB model showed a high pressure elastic instability (Cohen 1987a). Detailed PIB computations for different structures showed a phase transition at high pressures to the Rh_2O_3 II structure (Cynn et al. 1990), and the transition was confirmed and pressure computed accurately using the LAPW method with the PIB structural parameters (Marton and Cohen 1994). Pseudopotential calculations are in good agreement (Thompson et al. 1996). These computations predicted a phase transition near 90 GPa, in excellent agreement with later experiments (Funamori and Jeanloz 1997). The pseudopotential calculations predict a further transition to a perovskite phase at pressures above those found in the lower mantle (i.e. at 223 GPa).

Elastic moduli

The elastic moduli are of central importance in studies of the earth's interior since they govern the passage of seismic waves, our primary source of information on the structure of the subsurface. Despite their importance, density functional calculations of the elastic constants of earth materials have appeared only recently. The key development has been that of an efficient structural optimization scheme (Wentzcovitch et al. 1993), and calculation of stresses from the Hellman-Feynman theorem. Elastic constants are determined by calculating the stress generated by deviatoric strains applied to the equilibrium structure as described above. It is straightforward to demonstrate that one is within the linear regime by performing the calculation at a variety of values of the strain magnitude and extrapolating to the limit of zero strain (Karki et al. 1997b). These calculations show that strains of the order of 1 % are appropriate for silicates and oxides. By carefully choosing the symmetry of the applied strain, it is possible to calculate all elements of the elastic constant tensor with a small number of different strains. For example, the three elastic constants of a cubic mineral can be determined from a single strain; four different strains have been used for orthorhombic minerals (9 independent elastic constants) (Silva et al. 1997).

The full elastic constant tensors of a number of silicates and oxides have been determined with the plane-wave pseudopotential method, including that of MgO periclase, $MgSiO_3$ perovskite, Mg_2SiO_4 forsterite and ringwoodite, and SiO_2 in the stishovite, $CaCl_2$, and columbite structures (Karki et al. 1997a,b,c; Kiefer et al. 1997, Silva et al. 1997, Wentzcovitch et al. 1993). Once the elastic constant tensor is determined, it is straightforward to calculate the elastic wave (seismic) velocities in any direction, the elastic anisotropy, and the seismic-wave velocities of isotropic aggregates. Results for silica (Fig. 11) show several interesting features: (1) the phase transition from stishovite to the $CaCl_2$ structure is associated with an elastic instability (c_{11}-c_{12}->0) that originates from the coupled octahedral rotation and basal plane shear that relates the two structures; (2) this elastic

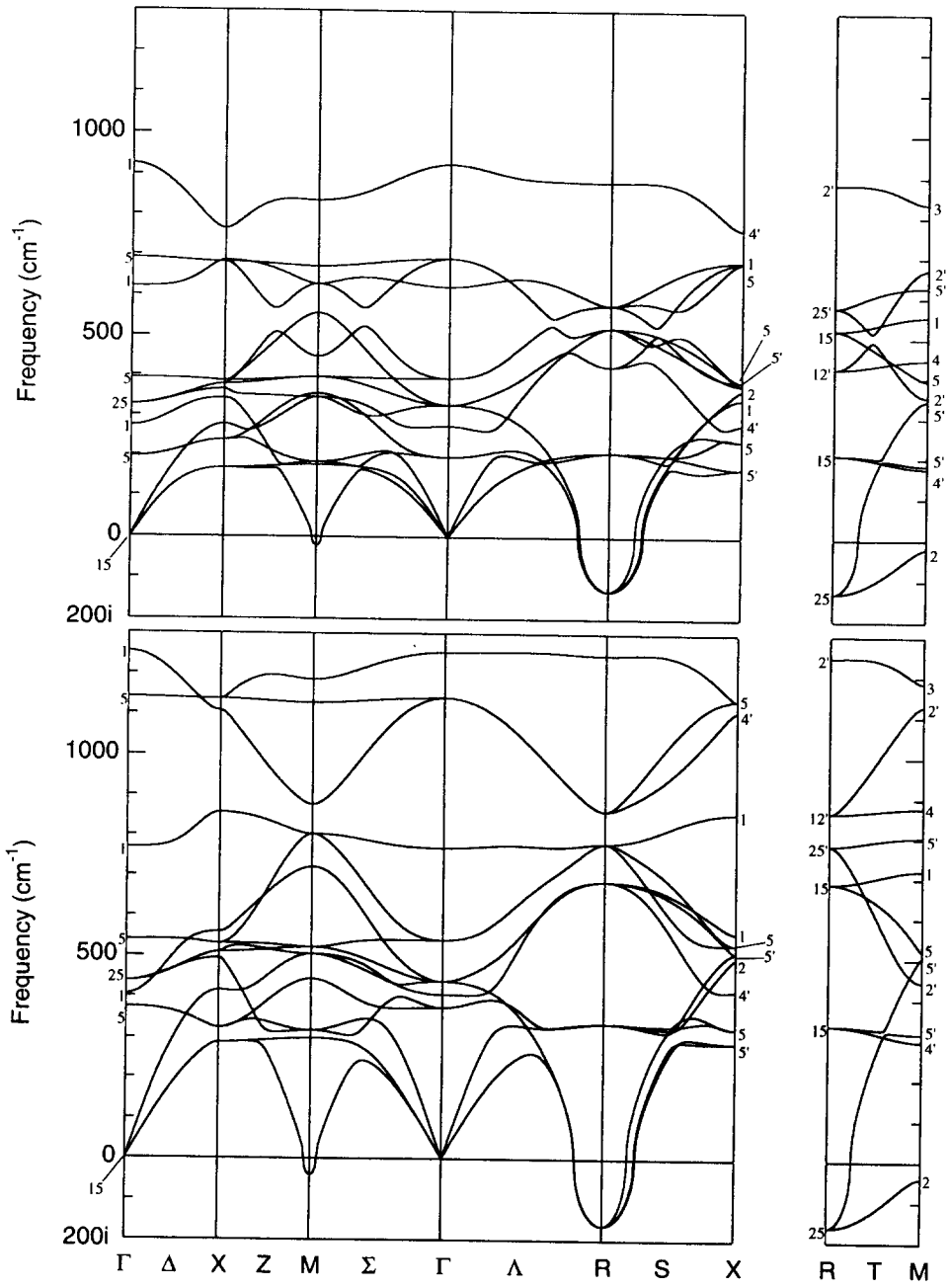

Figure 13. Phonon spectrum of the cubic phase at unit cell volume V = 310 Bohr^3 (P = -8 GPa) (a) compared with that at V = 240 Bohr^3 (P = 80 GPa) (b) (Stixrude et al. 1996). All zone-center modes (Γ-point) are stable. However, zone-boundary modes at the M- and R-points are unstable, as shown by the existence of imaginary frequencies. The final panel (M-R) shows that the edges of the cubic Brillouin zone are everywhere unstable. The magnitude of the imaginary eigenfrequencies increases with compression. Symmetry designations are those of Cowley (1964) as corrected by Boyer and Hardy (1981).

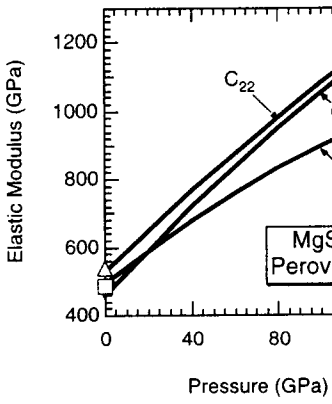

Figure 14. Elastic constants of MgSiO skite according to theory (Karki et al (lines) and experiment (Yeganeh-Haer Symbols: c_{11}, c_{12}, c_{44} (○)
c_{22}, c_{13}, c_{55} (△)
c_{33}, c_{23}, c_{66} (□)

instability is accompanied by a ve that it may be seismologically obse the earth's mantle, and (3) all ph anisotropy diverging in the neighb

Extensive computations have study because there are 20 atoms i than stishovite (Hemley and Cohe ionic model is not as successful a MgO, ab initio ionic models find p and alkaline earth oxides are foun 1986). For perovskite the predictio 1987b) were in reasonable agreem high-pressure elastic constants are scale computations of elastic con wave basis with pseudopotentials experiments is excellent, and th perovskite for pressures throughou computations of thermoelasticity a

Magnetic collapse

This phenomenon may occur high pressure and has been predic pressures above 100 GPa (Isaak et

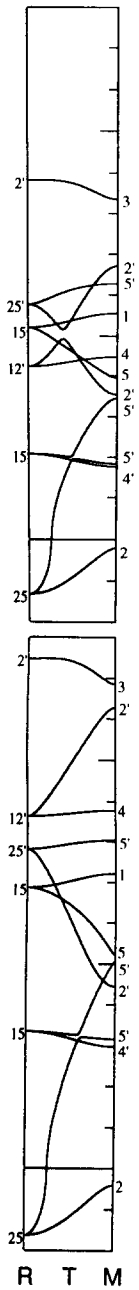

P = -8 GPa) (a) enter modes (Γ- shown by the Brillouin zone h compression.

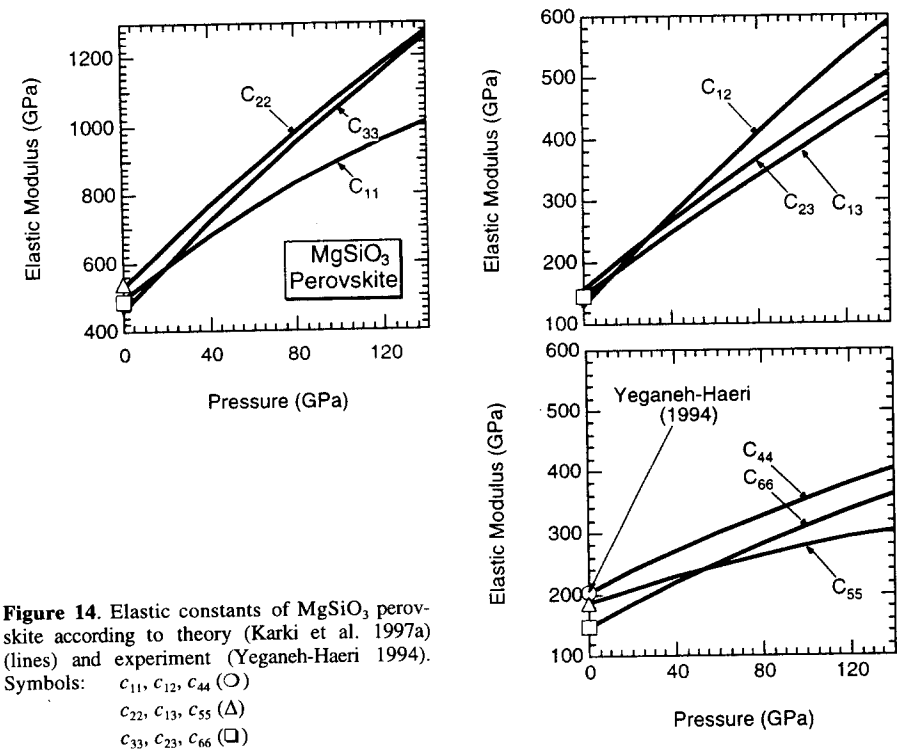

Figure 14. Elastic constants of $MgSiO_3$ perovskite according to theory (Karki et al. 1997a) (lines) and experiment (Yeganeh-Haeri 1994). Symbols: c_{11}, c_{12}, c_{44} (○) c_{22}, c_{13}, c_{55} (△) c_{33}, c_{23}, c_{66} (□)

instability is accompanied by a very large (60 %) change in shear wave velocity; so large that it may be seismologically observable if as little as a few percent of free silica exists in the earth's mantle, and (3) all phases of silica are highly anisotropic elastically with the anisotropy diverging in the neighborhood of the phase transition.

Extensive computations have been performed for $MgSiO_3$, although it is difficult to study because there are 20 atoms in the primitive unit cell. $MgSiO_3$ appears to be more ionic than stishovite (Hemley and Cohen 1992, Stixrude and Cohen 1993), but the fully charged ionic model is not as successful as it is for simple minerals such as MgO. In the case of MgO, ab initio ionic models find proper violations of the Cauchy relations in alkali halides and alkaline earth oxides are found which agree reasonably with experiment (Mehl et al. 1986). For perovskite the predictions of single crystal elastic constants for $MgSiO_3$ (Cohen 1987b) were in reasonable agreement with later experiments (Yeganeh-Haeri 1994), and high-pressure elastic constants are still not available experimentally. More recently, large scale computations of elastic constants have been performed for $MgSiO_3$ using a plane wave basis with pseudopotentials (Karki et al. 1997a) (Fig. 14). Agreement with available experiments is excellent, and these computations give predictions of the elasticity of perovskite for pressures throughout the mantle. These results will be benchmarks for future computations of thermoelasticity at mantle temperatures.

Magnetic collapse

This phenomenon may occur in a wide variety of transition metal bearing minerals at high pressure and has been predicted on the basis of first principles calculations in FeO at pressures above 100 GPa (Isaak et al. 1993) (Fig. 15). The predicted magnetic collapse is a

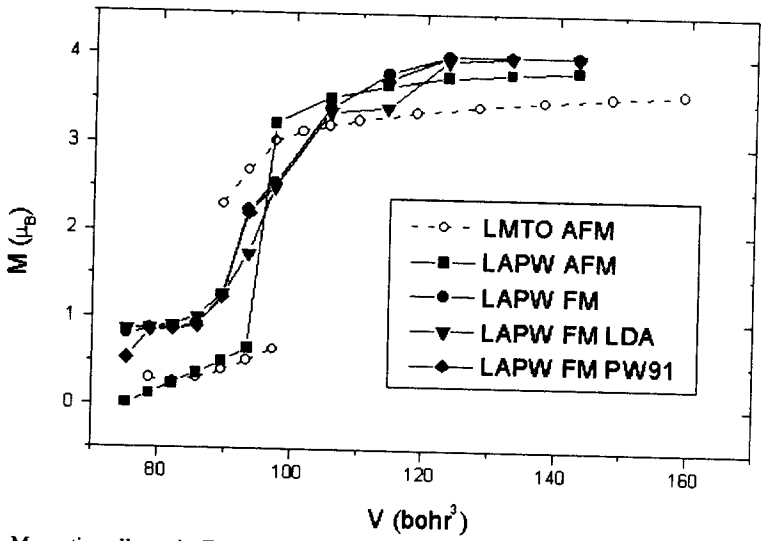

Figure 15. Magnetic collapse in FeO shown as a function of volume predicted from different levels of theory. FM and AFM correspond to ferromagnetic and antiferromagnetic calculations, and results are shown for both LAPW (linearized augmented plane wave) and LMTO (linearized muffin-tin orbital) methods. The generalized gradient approximation (GGA) results are labeled PW91. The high-spin/low spin transition is discontinuous in AFM and continuous in FM (Cohen et al. 1998).

type of high-spin low-spin transition, which has been observed in other materials such as NiI_2 and MnS . High-spin low-spin transitions can be either continuous higher-order phase transitions, or first-order phase transitions. Recent Mössbauer measurements indicated a 100 GPa transition in FeO (Pasternak et al. 1997), although recent x-ray K_β spectra show no transition to at least 130 GPa (see Hemley, Mao, and Cohen, this volume). More work is needed to understand these reported differences.

Magnetic collapse can be understood in terms of pressure-induced changes in the band structure with the Stoner model, discussed below. This picture contrasts with the conventional local atomic view which focuses only on the Brillouin zone center. In the conventional view, a high-spin to low-spin transition occurs when the crystal-field splitting between d orbitals of e_g and t_{2g} character exceeds the exchange splitting between up- and down-spin states (Burns 1993). Furthermore, the conventional view is that the e_g-t_{2g} splitting is due to the Coulomb potential from the transition metal atom's coordination polyhedron, and that the splitting increases as r_s^{-5}. Although reported crystal-field splittings vary approximately as r_s^{-5} in many cases, this view does not appear to be correct. In fact, the on-site contributions to the crystal field-splitting that arise from the electrostatic interaction with the surrounding O^{2-} ions have the wrong sign, and would give e_g lower than t_{2g} by a small amount, rather than t_{2g} being lower, as observed. Instead, the main contribution to the e_g-t_{2g} splitting is due to d-d hybridization between transition metal ions, which also varies as r_s^{-5}. These d-d interactions operate only at the Brillouin zone-center (Γ-point), also the only point where the e_g - t_{2g} symmetry is appropriate. At other points in the Brillouin zone, the band width is due to hybridization with O 2p states (Mattheiss 1972a,b). Optical spectroscopy measures not only the states at Γ, but rather is sensitive to vertical transitions throughout the zone, and thus to the entire bandwidth. The d-p interactions lead to a band width that behaves approximately as r_s^{-7}. Thus, the band width and apparent crystal field splitting should vary between r_s^{-5} and r_s^{-7} with increasing pressure. The distinction between the present picture and the conventional view can be seen

most easily in terms of the behavio
on-site, diagonal, elements that
splitting, whereas band theory says
change the band widths with press

The decrease in magnetism wi
sense in that as pressure increases
than the exchange splitting. This
(Cohen et al. 1997a). In the Stoner

$$\Delta E = \frac{-M^2 I}{2} + \frac{M^2}{2N(0)}$$

where M is the magnetic moment,
the density of states at the Fermi
state. The first-term is the exchar
change in the band energy with ma
to the Stoner criterion for a stable
being a property of the atom, rem
with increasing hybridization. In
changes in band topology at the F
decrease and disappear with increa

Mott insulators

Band theory is known to fail
often predicts metallic ground state
this failure may be similar to the fa
it is also believed that there is a mo
metal oxides, which is that LDA
between electrons of different angu
such orbital dependent potentials s
state charge density of a system, b
unknown, and would likely be e
density of transition metal oxide co
The main problem with LDA-like t
local Coulomb repulsion U, which
is added to an atom.

A promising method for real
needs further investigation is the I
1991, Mazin and Anisimov 1997).
simulate the effect of U. The para
energy with orbital occupancy in
excellent approximation at zero pr
unclear whether it will give reaso
smaller. The parameter U/W decr
pressure, but the band width increa
One explanation for the success of
in transition metal oxides discusse
making band theory more applica
transition metal oxides should be re

most easily in terms of the behavior of the Hamiltonian. In the conventional view, it is the on-site, diagonal, elements that vary rapidly with pressure, giving rise to increased splitting, whereas band theory says that it is the off-diagonal, covalent, contributions which change the band widths with pressure.

The decrease in magnetism with increasing pressure can be understood in a qualitative sense in that as pressure increases, band widths increase, and eventually become greater than the exchange splitting. This can be examined quantitatively with the Stoner model (Cohen et al. 1997a). In the Stoner model, the effect of magnetism on the total energy is

$$\Delta E = \frac{-M^2 I}{2} + \frac{M^2}{2N(0)} \tag{23}$$

where M is the magnetic moment, the Stoner Integral I is an atomic property, and $N(0)$ is the density of states at the Fermi level (or top of the valence band) in the non-magnetic state. The first-term is the exchange energy due to magnetization and the second is the change in the band energy with magnetic moment. Minimizing ΔE with respect to M leads to the Stoner criterion for a stable magnetic state, $IN(0) > 1$. As pressure is increased I, being a property of the atom, remains constant but $N(0)$ decreases as band widths widen with increasing hybridization. In the absence of new bands crossing the Fermi level or changes in band topology at the Fermi level or top of the valence band, magnetism will decrease and disappear with increasing pressure.

Mott insulators

Band theory is known to fail in the case of transition metal oxides in the sense that it often predicts metallic ground states when these are observed to be insulating. The cause of this failure may be similar to the failure to predict accurate band gaps in other materials, but it is also believed that there is a more specific failure of LDA-like theories for the transition metal oxides, which is that LDA is local, as discussed above, and does not distinguish between electrons of different angular momentum. The Hohenberg-Kohn theorem says that such orbital dependent potentials should not be necessary to find the energy and ground-state charge density of a system, but the exact functional that would give this behavior is unknown, and would likely be extremely complex in order to give the proper charge density of transition metal oxide compounds, especially those that involve orbital ordering. The main problem with LDA-like theories is believed to be the mean-field treatment of the local Coulomb repulsion U, which is a measure of the increase in energy when an electron is added to an atom.

A promising method for realistic computations of real Mott insulators, but which needs further investigation is the LDA+U model (Anisimov et al. 1993, Anisimov et al. 1991, Mazin and Anisimov 1997). In this method an orbital dependent potential is added to simulate the effect of U. The parameter U can be estimated by computing the change in energy with orbital occupancy in constrained LDA calculations. LDA+U appears to be an excellent approximation at zero pressure where the band width (W) is small, but it is unclear whether it will give reasonable results at high pressures, where U/W is much smaller. The parameter U/W decreases with pressure since U is relatively insensitive to pressure, but the band width increases rapidly with pressure due to increased hybridization. One explanation for the success of band theory in the case of the high pressure transitions in transition metal oxides discussed above is that U/W is small under at high pressure, making band theory more applicable and predictive. Transitions predicted for the other transition metal oxides should be re-examined.

High-temperature and transport properties

The effect of temperature is directly linked to the dynamics of a crystal: thermal contributions can be written as a sum over lattice vibrations (phonons). Because dynamics break the symmetry of the primitive unit cell, determination of dynamics from first principles is a substantial computational challenge. This can be accomplished either by determining the dynamical matrix and diagonalizing to find the phonon frequencies (e.g. via linear response, discussed above), or by molecular dynamics, a brute force approach which simply solves Newton's equations of motion for a periodic array of nuclei. Molecular dynamics has the advantage of also being able to treat transport properties such as chemical diffusivity, and liquids. Nearly all previous studies of vibrations, high temperature properties, or transport properties have been based on semi-empirical or ab initio methods. Molecular dynamics simulations using the pseudopotential method have now been performed on deep earth materials for the first time in a study of liquid iron at core conditions (Wijs et al. 1998). The first-principles investigation of other solid and fluid earth materials by this technique represents an exciting future direction.

The biggest advantage of fast, ab initio methods such as PIB or VIB is that one can perform lattice dynamics and long molecular dynamics simulations on systems of reasonable size, and study a wide variety of thermodynamic and transport properties. For example, Isaak et al. (1990) performed lattice dynamics on MgO as a function of lattice strain, going beyond the normal quasiharmonic approximation, and studied the effects of temperature and pressure on elasticity and the equation of state. In that study, the dynamical matrix was found throughout the Brillouin zone in order to obtain the free energy, and this was repeated for different lattice strains. In spite of increased computational power in the last eight years, no such study has yet been done self-consistently. The Isaak et al. study gave what are still one of the few estimates of cross derivatives of pressure and temperature on elasticity that are available. The results were then used to help understand the increase in seismic parameter $d\ln V_s / d\ln V_p$ with depth in the Earth, a quantity that has been difficult to constrain experimentally.

Going beyond lattice dynamics, Inbar and Cohen (1995) determined the thermal equation of state of MgO using molecular dynamics and the PIB model. Such studies are just becoming possible using self-consistent methods, and still have not been performed. Using molecular dynamics and the VIB model, it is also possible to study complex phenomena, such as thermal conductivity (Cohen 1998) and diffusion (Ita and Cohen 1997, 1998). The diffusivity of O in MgO, for example, is obtained in agreement with measurements within experimental error.

Because high temperature properties are difficult to obtain self-consistently, Wasserman et al. (1996) applied the particle-in-a-cell model to compute thermodynamic properties of iron at high pressures and temperatures in conjunction with a new fast and accurate tight-binding model (discussed above in the tight binding section) that allows computations for large unit cells (Cohen et al. 1994). They obtained excellent agreement with shock compression data up to ultrahigh pressures and temperatures (Stixrude et al. 1997). They also performed molecular dynamics using the tight-binding model for iron liquid at outer core conditions (Fig. 16), and obtained an estimate of the viscosity of liquid iron in excellent agreement with subsequent pseudopotential calculations (Wijs et al. 1998). These results are geophysically significant because the viscosity of the outer core had been uncertain by 13 orders of magnitude.

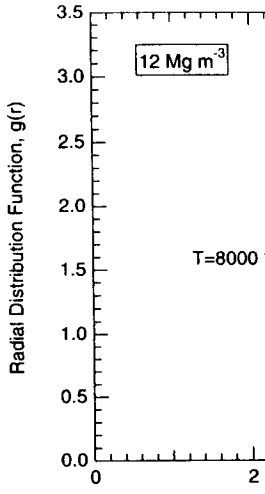

Figure 16. Radial distribution function c
bottom of the earth's outer core. Calcul
binding total energy method of Cohen et
from these simulations is 5(±3) centipois

CONCL

Modern first-principles meth
experimentally observable proper
stability, crystal structure, and el
experiment, these methods have
features such as phase transitions
principles methods including dens
the experimental approach towards
conditions. This review has only g
condensed-matter theory to the stu
a subset of the important calculati
progress on a number of fronts
interplay of theory and experiment

AC

This work supported by the N
EAR-9614790, and EAR-972
EAR-9614363 (REC); EAR-97
The computations at the Geophysi
which is supported by NSF grant
Institution of Washington.

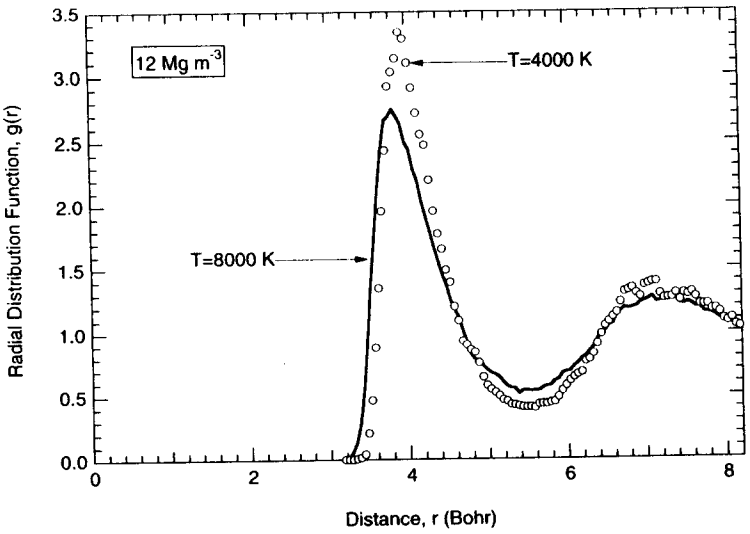

Figure 16. Radial distribution function of liquid iron at two temperatures at a density corresponding to the bottom of the earth's outer core. Calculations were perfomed via molecular dynamics based on the tight-binding total energy method of Cohen et al. (Cohen et al. 1994). The Stokes-Einstein viscosity calculated from these simulations is 5(±3) centipoise, and is weakly dependent on temperature over the range shown.

CONCLUSIONS AND OUTLOOK

Modern first-principles methods are now capable of realistic predictions of many experimentally observable properties of minerals such as the equation of state, phase stability, crystal structure, and elasticity. Parameter-free and completely independent of experiment, these methods have been shown to reproduce observations even of subtle features such as phase transitions and the elastic anisotropy with good accuracy. First-principles methods including density functional theory represent the ideal complement to the experimental approach towards studying the behavior of earth materials under extreme conditions. This review has only given an indication of the realm of application of modern condensed-matter theory to the study of minerals at high pressure. We have reviewed only a subset of the important calculations that have been performed. One foresees accelerated progress on a number of fronts in this challenging field resulting from the continued interplay of theory and experiment.

ACKNOWLEDGMENTS

This work supported by the National Science Foundation under grants EAR-9628199, EAR-9614790, and EAR-9729194 (LPS); EAR-9305060, EAR-9870328, and EAR-9614363 (REC); EAR-9710475, EAR-9526763 and EAR-9706624 (RJH). The computations at the Geophysical Laboratory were performed on a Cray J90/16-4096, which is supported by NSF grant EAR-9512627, the Keck Foundation, and the Carnegie Institution of Washington.

REFERENCES

Anderson OK (1975) Linear methods in band theory. Phys Rev B 12:3060-3083

Anisimov VI, Solovyev IV, Korotin MA, Czyzyk MT, Sawatzky GA (1993) Density functional theory and NiO photoemission spectra. Phys Rev B 48:16929-16934

Anisimov VI, Zaanen J, Andersen OK (1991) Band theory and Mott insulators: Hubbard U instead of Stoner U. Phys Rev B 44:943-954

Bagno P, Jepsen O, Gunnarson O (1989) Ground-state properties of third-row elements with nonlocal density functionals. Phys Rev B 40:1997-2000

Baroni S, Giannozzi P, Testa A (1987) Green-function approach to linear response in solids. Phys Rev Lett 58:1861-1864

Birch F (1952) Elasticity and constitution of the earth's interior. J Geophys Res 57:227-286

Boyer LL, Hardy JR (1981) Theoretical study of the structural phase transition in $RbCaF_3$. Phys Rev B 24:2577-2591

Boyer LL et al. (1985) Beyond the rigid ion approximation with sphercally symmetric ions. Phys Rev Lett 54:1940-1943

Boyer LL, Stokes HT, Mehl MJ (1997) Application of a Kohn-Sham-like formulation of the self-consistent atomic deformation model. Ferroelec 194:173-186

Bukowinski MST (1977) A theoretical equation of state for the inner core. Phys Earth Planetary Inter 14:333-344

Bukowinski MST (1985) First principles equations of state of MgO and CaO. Geophys Res Lett 12:536-539

Bukowinski MST (1994) Quantum geophysics. Ann Rev Earth Planet Sci 22:167-205

Burnham CW (1990) The ionic model: Perceptions and realities in mineralogy. Am Mineral 75:443-463

Burns RG (1993) Mineralogical Applications of Crystal Field Theory. Cambridge University Press, Cambridge

Ceperley DM, Alder BJ (1980) Ground state of the electron gas by a stochastic method. Phys Rev Lett 45:566-569

Chabrier G (1992) The molecular-metallic transition of hydrogen and the structure of Jupiter and Saturn. Astrophys J 391:817-826

Cohen AJ, Gordon RG (1975) Theory of the lattice energy, equilibrium structure, elastic constants, and pressure-induced phase transformations in alkali-halides. Phys Rev B 12:3228-3241

Cohen AJ, Gordon RG (1976) Modified electron-gas study of the stability, elastic properties, and high-pressure behavior of MgO and CaO crystals. Phys Rev B 14:4593-4605

Cohen RE (1987a) Calculation of elasticity and high pressure instabilities in corundum and stishovite with the potential induced breathing model. Geophys Res Lett 14:37-40

Cohen RE (1987b) Elasticity and equation of state of $MgSiO_3$ perovskite. Geophys Res Lett 14:1053-1056

Cohen RE (1991) Bonding and elasticity of stishovite SiO_2 at high pressure: linearized augmented plane wave calculations. Am Mineral 76:733-742

Cohen RE (1992) First-principles predictions of elasticity and phase transitions in high pressure SiO_2 and geophysical implications. In: Y. Syono and M.H. Manghnani (eds) High-Pressure Research: Applications to Earth and Planetary Sciences, p 425-431 Terrapub, Tokyo

Cohen, R.E (1998) Thermal conductivity of MgO at high pressures. In: M Nakahara (ed) Review of High-Pressure Science and Technology 7:160-162, Japan Soc. High-Pres Science Technol., Kyoto, Japan

Cohen RE, Boyer LL, Mehl MJ (1987) Lattice dynamics of the potential induced breathing model: First principles phonon dispersion in the alkaline earth oxides. Phys Rev B 35:5749-5760

Cohen RE, Mazin II, Isaak DG (1997a) Magnetic collapse in transition metal oxides at high pressure: Implications for the Earth. Science 275:654-657

Cohen RE, Mehl MJ, Papaconstantopoulos DA (1994) Tight-binding total-energy method for transition and noble metals. Phys Rev B 50:14694-14697

Cohen RE, Stixrude L, Wasserman E (1997b) Tight-binding computations of elastic anisotropy of Fe, Xe, and Si under compression. Phys Rev B 56:8575-8589

Cohen RE, Fei Y, Downs R, Mazin II, Isaak DG (1998) Magnetic collapse and the behavior of transition metal oxides: FeO at high pressures. In: Wentzcovitch R, Hemley RJ, Nellis WJ, Yu P (eds) High-Pressure Materials Research. Proceedings of the Fall 1997 Materials Research Society Meeting, Vol 499 Pittsburgh, PA in press

Cowley R (1964) Lattice dynamics and phase transitions of strontium titanate. Phys Rev 134:A981-A997

Cynn H, Isaak DG, Cohen RE, Nicol MF, Anderson OL (1990) A high pressure phase transition of corundum predicted by the Potential Induced Breathing model. Am Mineral 75:439

Dovesi R, Pisani C, Roetti C, Silvi B (1987) The electronic structure of α-quartz: A periodic Hartree-Fock calculation. J Chem Phys 86:6967-6971

Duffy TS, Hemley RJ, Mao HK (1
pressures—magnesium oxide to 227

Dziewonski AM, Anderson DL (1981) Pr
356

Edwardson PJ (1989) Corridors-between-a
63:55-59

Funamori N, Jeanloz R (1997) High press

Gell-Mann M, Brueckner KA (1957) Corr
106:364-368

Gordon RG, Kim YS (1972) Theory
J Chem.Phys. 56:3122-3133

Gunnarsson O, Lundqvist BI (1976) Excha
density-functional formalism. Phys R

Harrison WA (1989) Electronic structure a

Hedin L, Lundqvist BI (1971) Explicit lo
4:2064-2083

Hemley RJ, Cohen RE (1992) Silicate pe

Hemley RJ, Jackson MD, Gordon RG (19
to high pressures and temperatures: a

Hemley RJ, Jackson MD, Gordon RG
equations of state of perovskite-type

Hemley RJ, Prewitt CT, Kingma KJ (199

Hohenberg P, Kohn W (1964) Inhomogen

Hubbard WB (1984) Planetary Interiors. V

Ichimaru S (1982) Strongly coupled plasm
Rev Mod Phys 54:1017-1059

Inbar I, Cohen RE (1995) High pressure e
1536

Isaak DG, Cohen RE, Mehl MJ (1990) C
and Temperatures. J Geophys Res 95:

Isaak DG, Cohen RE, Mehl MJ, Singh
principles linearized augmented plane

Ita J, Cohen RE (1997) Effects of pressure
free-energy integrations. Phys Rev Le

Ita J, Cohen RE (1998) Diffusion in M
Geophys Res Lett 25:1095-1098

Jensen H (1938) Das Druck-Dichte Diagra
Zeits Phys 111:373-385

Karki BB, Stixrude L, Clark SJ, Warren
rhombic $MgSiO_3$ perovskite at lower

Karki BB, Stixrude L, Clark SJ, Warren M
at high pressure. Am Mineral 82:51-6

Karki BB, Stixrude L, Warren MC, Ackla
polymorphs of silica. Geophys Res L

Karki BB, Warren MC, Stixrude L, Ac
structural transformations in silica. P

Karki BB, Warren MC, Stixrude L, Ac
structural transformations in silica (e

Kiefer B, Stixrude L, Wentzcovitch R
normal and inverse ringwoodite. Am

Kiefer B, Stixrude L, Wentzcovitch RM
pressure. Geophys Res Lett 24:2841-

Kingma K, Mao HK, Hemley RJ (1996)
High Press Res 14:363-374

Kingma KJ, Cohen RE, Hemley RJ, Mac
mantle pressures. Science 374:243-24

Knittle E, Jeanloz R (1987) Synthesis
gigapascals. Science 235:668-670

Kohan AF, Ceder G (1996) Tight-bindi
application to the MgO-CaO phase d

Duffy TS, Hemley RJ, Mao HK (1995) Equation of state and shear-strength at multimegabar pressures—magnesium oxide to 227 GPa. Phys Rev Lett 74:1371-1374
Dziewonski AM, Anderson DL (1981) Preliminary reference earth model. Phys Earth Planet Inter 25:297-356
Edwardson PJ (1989) Corridors-between-adjacent-sites model for the four phases of $KNbO_3$. Phys Rev Lett 63:55-59
Funamori N, Jeanloz R (1997) High pressure transformation of Al_2O_3. Science 278:1109-1111
Gell-Mann M, Brueckner KA (1957) Correlation energy of an electron gas at high density. Physical Review 106:364-368
Gordon RG, Kim YS (1972) Theory for the forces between closed-shell atoms and molecules. J Chem.Phys. 56:3122-3133
Gunnarsson O, Lundqvist BI (1976) Exchange and correlation in atoms, molecules, and solids by the spin-density-functional formalism. Phys Rev B 13:4274-4298
Harrison WA (1989) Electronic structure and the properties of solids. Dover, New York
Hedin L, Lundqvist BI (1971) Explicit local exchange-correlation potentials. J Phys C:Solid State Phys 4:2064-2083
Hemley RJ, Cohen RE (1992) Silicate perovskite. Ann Rev Earth Planet Sci 20:553-600
Hemley RJ, Jackson MD, Gordon RG (1985) First-principles theory for the equations of state of minerals to high pressures and temperatures: application to MgO. Geophys Res Lett 12:247-250
Hemley RJ, Jackson MD, Gordon RG (1987) Theoretical study of the structure, lattice dynamics, and equations of state of perovskite-type $MgSiO_3$. Phys Chem Minerals 14:2-12
Hemley RJ, Prewitt CT, Kingma KJ (1994) High-pressure behavior of silica. Rev Mineral 29:41-81
Hohenberg P, Kohn W (1964) Inhomogeneous electron gas. Phys Rev 136:B864-B871
Hubbard WB (1984) Planetary Interiors. Van Nostrand Reinhold, New York
Ichimaru S (1982) Strongly coupled plasmas: high-density classical plasmas and degenerate electron liquids. Rev Mod Phys 54:1017-1059
Inbar I, Cohen RE (1995) High pressure effects on thermal properties of MgO. Geophys Res Lett 22:1533-1536
Isaak DG, Cohen RE, Mehl MJ (1990) Calculated elastic and thermal properties of MgO at high pressure and Temperatures. J Geophys Res 95:7055-7067
Isaak DG, Cohen RE, Mehl MJ, Singh DJ (1993) Phase stability of wüstite at high-pressure from 1st-principles linearized augmented plane-wave calculations. Phys Rev B 47:7720-7731
Ita J, Cohen RE (1997) Effects of pressure on diffusion and vacancy formation in MgO from non-empirical free-energy integrations. Phys Rev Lett 79:3198-3201
Ita J, Cohen RE (1998) Diffusion in MgO at high pressure: Implications for lower mantle rheology. Geophys Res Lett 25:1095-1098
Jensen H (1938) Das Druck-Dichte Diagramm der Elemente bei höheren Drucken am Temperaturnullpunkt. Zeits Phys 111:373-385
Karki BB, Stixrude L, Clark SJ, Warren MC, Ackland GJ, Crain J (1997a) Elastic Properties of orthorhombic $MgSiO_3$ perovskite at lower mantle pressures. Am Mineral 82:635-638
Karki BB, Stixrude L, Clark SJ, Warren MC, Ackland GJ, Crain J (1997b) Structure and elasticity of MgO at high pressure. Am Mineral 82:51-60
Karki BB, Stixrude L, Warren MC, Ackland GJ, Crain J (1997c) Ab initio elasticity of three high-pressure polymorphs of silica. Geophys Res Lett 24:3269-3272
Karki BB, Warren MC, Stixrude L, Ackland GJ, Crain J (1997d) Ab initio studies of high-pressure structural transformations in silica. Phys Rev B 55:3465-3471
Karki BB, Warren MC, Stixrude L, Ackland GJ, Crain J (1997e) Ab initio studies of high-pressure structural transformations in silica (erratum, vol 55, pg 3465, 1997). Phys Rev B 56:2884-2884
Kiefer B, Stixrude L, Wentzcovitch R (1998) Ab initio investigation of structure and compression in normal and inverse ringwoodite. Am Mineral (in press)
Kiefer B, Stixrude L, Wentzcovitch RM (1997) Elastic constants and anisotropy of Mg_2SiO_4 spinel at high pressure. Geophys Res Lett 24:2841-2844
Kingma K, Mao HK, Hemley RJ (1996) Synchrotron x-ray diffraction of SiO_2 to multimegabar pressures. High Press Res 14:363-374
Kingma KJ, Cohen RE, Hemley RJ, Mao HK (1995) Transformation of silica to a denser phase at lower-mantle pressures. Science 374:243-245
Knittle E, Jeanloz R (1987) Synthesis and equation of state of $(Mg,Fe)SiO_3$ perovskite to over 100 gigapascals. Science 235:668-670
Kohan AF, Ceder G (1996) Tight-binding calculation of formation energies in multicomponent oxides: application to the MgO-CaO phase diagram. Phys Rev B 54:805-811

Kohn W, Sham LJ (1965) Self-consistent equations including exchange and correlation effects. Phys Review 140:A1133-A1138
Körling M, Häglund J (1992) Cohesive and electronic properties of transition metals: The generalized gradient approximation. Phys Rev B 45:13293-13297
Lee C, Gonze X (1995) Ab-initio calculation of the thermodynamic properties and atomic temperature factors of SiO_2 alpha-quartz and stishovite. Phys Rev B 51:8610-8613
LeSar R (1983) Phys Rev B 28:6812
LeSar R (1988) Equations of state of dense helium. Phys Rev Lett 61:2121-2124
Lin JS, Qteish Q, Payne MC, Heine V (1993) Optimised and transferable non-local separable ab-initio pseudopotentials. Phys Rev B 47:4174-4180
Lundqvist S, March NH (1987) Theory of the Inhomogeneous Electron Gas. Plenum Press, London
Mao HK et al. (1991) Effect of pressure, temperature, and composition on lattice parameters and density of $(Fe,Mg)SiO_3$ perovskites to 30 GPa. J Geophys Res 96:8069-8079
Mao HK, Wu Y, Chen LC, Shu JF, Jephcoat AP (1990) Static compression of iron to 300 GPa and $Fe_{0.8}Ni_{0.2}$ alloy to 260 GPa: Implications for composition of the core. J Geophys Res 95:21737-21742
Marton FC, Cohen RE (1994) Prediction of a high pressure phase transition in Al_2O_3. Am Mineral 79:789-792
Mattheiss LF (1972a) Electronic structure of the 3d transition -metal monoxides. II. Interpretation. Phys Rev B 5:306-315
Mattheiss LF (1972b) Electronic structure of the 3d transition-metal monoxides. I. Energy-band results. Phys Rev B 5:290-306
Mazin II, Anisimov VI (1997) Insulating gap in FeO: Correlations and covalency. Phys Rev B 55: 12822-12825
Mehl MJ, Cohen RE, Krakauer H (1988) Linearized augmented plane wave electronic structure calculations for MgO and CaO. J Geophy Res 93:8009-8022
Mehl MJ, Hemley RJ, Boyer LL (1986) Potential induced breathing model for the elastic moduli and high-pressure behavior of the cubic alkaline-earth oxides. Phys Rev B 33:8685-8696
Monkhurst HJ, Pack JD (1976) Special points for Brillouin-zone integrations. Phys Rev B 13:5188-5192
Muhlhausen C, Gordon RG (1981) Electron-gas theory of ionic crystals, including many-body effects. Phys Rev B 23:900-923
Nielsen OH, Martin R (1985) Quantum mechanical theory of stress and force. Phys Rev B 32:3780-3791
Pasternak MP et al. (1997) High pressure collapse of magnetism in $Fe_{0.94}O$: Mössbauer spectroscopy beyond 100 GPa. Phys Rev Lett 79:5046-5049
Pauling L (1960) The Nature of the Chemical Bond. Cornell University Press, Ithaca, New York
Perdew JP, Burke K, Ernzerhof M (1996) Generalized gradient approximation made simple. Phys Rev Lett 77:3865-3868
Perdew JP et al. (1992) Atoms, molecules, solids, and surfaces—application of the generalized gradient approximation for exchange and correlation. Phys Rev B 46:6671-6687
Perdew JP, Zunger A (1981) Self-interaction correction to density-functional approximations for many-electron systems. Phys Rev B 23:5048-5079
Pickett WE (1989) Pseudopotentials in condensed matter systems. Comput Phys Rep 9:114-197
Sherman DM (1997) The composition of the earth's core: constraints on S and Si vs. temperature. Earth Planet Sci Lett 153:149-155
Sigalas M, Papaconstantopoulos DA, Bacalis NC (1992) Total energy and band structure of the 3d, 4d, and 5d metals. Phys Rev B 45:5777-5783
Silva Cd, Stixrude L, Wentzcovitch RM (1997) Elastic constants and anisotropy of forsterite at high pressure. Geophys Res Lett 24:1963-1966
Singh DJ (1994) Planewaves, Pseudopotentials, and the LAPW Method. Kluwer Academic, Norwall, Massachusetts
Slater JC (1951) A simplification of the Hartree-Fock method. Phys Rev 81:385-390
Slater JC, Koster GF (1954) Simplified LCAO method for the periodic potential problem. Phys Rev 94:1498-1524
Söderlind P, Moriarty JA, Willis JM (1996) First-principles theory of iron up to earth-core pressures: structural, vibrational, and elastic properties. Phys Rev B 53:14063-14072
Stixrude L, Cohen RE (1993) Stability of orthorhombic $MgSiO_3$-perovskite in the Earth's lower mantle. Nature 364:613-616
Stixrude L, Cohen RE (1995) Constraints on the crystalline structure of the inner core: Mechanical instability of BCC iron at high pressure. Geophys Res Lett 22:125-128
Stixrude L, Cohen RE, Singh DJ (1994) Iron at high pressure: linearized augmented plane wave calculations in the generalized gradient approximation. Phys Rev B 50:6442-6445
Stixrude L, Cohen RE, Yu RC, Krakauer H implications for lower mantle structure
Stixrude L, Wasserman E, Cohen RE (1997 Res 102:24729-24739
Stokes HT, Boyer LL, Mehl MJ (1996) principles energy calculations in ionic
Teter DM, Hemley RJ, Kresse G, Hafner J 80:2145-2148
Thompson KT, Wentzcovitch RM, Bukov principles: Putting pressure on the ruby
Troullier N, Martins JL (1991) Efficien 43:1993-2003
Vanderbilt D (1990) Soft self-consistent ps B 41:7892-7895
Wallace DC (1972) Thermodynamics of Cr
Wasserman E, Stixrude L, Cohen RE (199 Phys Rev B 53:8296-8309
Watson RE (1958) Analytic Hartree-Fock
Wei SH, Krakauer H (1985) Local-density BaSe and BaTe. Phys Rev Lett 55:120
Weidner DJ, Bass JD, Ringwood AE, Sin J Geophys Res 87:4740-4746
Wentzcovitch RM (1991) Invariant molecu B 44:2358-2361
Wentzcovitch RM, Hugh-Jones DA, Ang enstatite. Phys Chem Minerals 22:453
Wentzcovitch RM, Martins JL, Price GD application to $MgSiO_3$ perovskite. Ph
Wentzcovitch RM, Ross NL, Price GD (lower-mantle pressures. Phys Earth Pl
Wentzcovitch RM, Silva Cd, Chelikows amorphization in silica. Phys Rev Let
Wentzcovitch RM, Stixrude L (1997) Crys 82:663-671
Wigner E (1934) On the interaction of elec
Wijs GAd et al. (1998) The viscosity of 392:805-807
Wolf GH, Bukowinski MST (1987) Theor $MgSiO_3$ and $CaSiO_3$ perovskites: im and Y. Syono (eds) High Pressure Res
Wolf GH, Bukowinski MST (1988) Varia gas theory of crystals: Applications to
Yeganeh-Haeri A (1994) Synthesis and re- silicate perovskite. Phys Earth Planet

Stixrude L, Cohen RE, Yu RC, Krakauer H (1996) Prediction of phase transition in $CaSiO_3$ perovskite and implications for lower mantle structure. Am Mineral 81:1293-1296
Stixrude L, Wasserman E, Cohen RE (1997) Composition and temperature of earth's inner core. J Geophys Res 102:24729-24739
Stokes HT, Boyer LL, Mehl MJ (1996) Spherical self-consistent atomic deformation model for first-principles energy calculations in ionic crystalline solids. Phys Rev B 54:7729-7736
Teter DM, Hemley RJ, Kresse G, Hafner J (1998) High pressure polymorphism in silica. Phys Rev Lett 80:2145-2148
Thompson KT, Wentzcovitch RM, Bukowinski MST (1996) Polymorphs of alumina predicted by first principles: Putting pressure on the ruby scale. Science 274:1880-1882
Troullier N, Martins JL (1991) Efficient pseudopotentials for plane-wave calculations. Phys Rev B 43:1993-2003
Vanderbilt D (1990) Soft self-consistent pseudopotentials in a generalized eigenvalue formalism. Phys Rev B 41:7892-7895
Wallace DC (1972) Thermodynamics of Crystals. John Wiley & Sons, New York
Wasserman E, Stixrude L, Cohen RE (1996) Thermal properties of iron at high pressures and temperatures. Phys Rev B 53:8296-8309
Watson RE (1958) Analytic Hartree-Fock solutions for O^{2-}. Phys Rev 111:1108-1110
Wei SH, Krakauer H (1985) Local-density-functional calculations of the pressure-induced metallization of BaSe and BaTe. Phys Rev Lett 55:1200-1203
Weidner DJ, Bass JD, Ringwood AE, Sinclair W (1982) The single-crystal elastic moduli of stishovite. J Geophys Res 87:4740-4746
Wentzcovitch RM (1991) Invariant molecular dynamics approach to structural phase transitions. Phys Rev B 44:2358-2361
Wentzcovitch RM, Hugh-Jones DA, Angel RJ, Price GD (1995a) Ab initio study of $MgSiO_3$ *C2/c* enstatite. Phys Chem Minerals 22:453-460
Wentzcovitch RM, Martins JL, Price GD (1993) Ab initio molecular dynamics with variable cell shape: application to $MgSiO_3$ perovskite. Phys Rev Lett 70:3947-3950
Wentzcovitch RM, Ross NL, Price GD (1995b) Ab initio study of $MgSiO_3$ and $CaSiO_3$ perovskites at lower-mantle pressures. Phys Earth Planet Inter 90:101-112
Wentzcovitch RM, Silva Cd, Chelikowsky JR, Binggeli N (1998) A new phase and pressure induced amorphization in silica. Phys Rev Lett 80:2149-2152
Wentzcovitch RM, Stixrude L (1997) Crystal chemistry of forsterite: a first principles study. Am Mineral 82:663-671
Wigner E (1934) On the interaction of electrons in metals. Phys Rev 46:1002-1011
Wijs GAd et al. (1998) The viscosity of liquid iron at the physical conditions of the earth's core. Nature 392:805-807
Wolf GH, Bukowinski MST (1987) Theoretical study of the structural properties and equations of state of $MgSiO_3$ and $CaSiO_3$ perovskites: implications for lower mantle composition. In: M.H. Manghnani and Y. Syono (eds) High Pressure Research in Mineral Physics, p 313-331 Terrapub, Tokyo
Wolf GH, Bukowinski MST (1988) Variational stabilization of the ionic charge densities in the electron-gas theory of crystals: Applications to MgO and CaO. Phys Chem Minerals 15:209-220
Yeganeh-Haeri A (1994) Synthesis and re-investigation of the elastic properties of single-crystal magnesium silicate perovskite. Phys Earth Planet Inter 87:111-121